

BEARING TESTER DATA COMPILATION
ANALYSIS, AND REPORTING AND
BEARING MATH MODELING

QUARTERLY PROGRESS REPORT
FOR
JULY - SEPTEMBER, 1985

SUBMITTED BY: SRS Technologies
555 Sparkman Drive, Suite 1406
Huntsville, AL 35805

PREPARED FOR: Mr. Fred J. Dolan
Materials and Processes Laboratory
Engineering Physics Division
George C. Marshall Space Flight Center
Marshall Space Flight Center

CONTRACT NUMBER: NAS8-36183



SYSTEMS TECHNOLOGY DIVISION

555 SPARKMAN DRIVE SUITE 1406
HUNTSVILLE, ALABAMA 35805
(205) 830-0375

SRS Technologies

FOREWORD

This quarterly report was prepared by SRS Technologies under Contract No. NAS8-36183 for the George C. Marshall Space Flight Center of the National Aeronautics and Space Administration. The work was administered under the technical direction of the Materials and Processes Laboratory, Engineering Physics Division with Mr. Fred J. Dolan acting as project manager.

This report describes the work performed by SRS Technologies during the third quarter of 1985 (July through September). Mr. Joe C. Cody served as the SRS Technologies Principle Investigator. The SRS project personnel who made major contributions to this report include:

Alok Majumdar

David Marty

Bruce Tiller.

SRS Technologies

CONTENTS

SECTION	PAGE
1.0 SUMMARY	1
2.0 SYNOPSIS OF PREVIOUS REPORTS.	3
3.0 WORK PERFORMED DURING CURRENT REPORTING PERIOD.	5
3.1 Cage Loads from Coolant Jets and Fluid Friction.	5
3.2 Viscous Heat Generation from Fluid Friction & Pumping.	9
3.3 LOX Turbopump Turbine End Bearing Thermal Investigation.	9
3.4 Coolant Flow Diverter Velocities	13
3.5 Contact Angles & Ball Tracks as Function of Bearing Load	24
3.6 Status of Bearing Modeling Program ADORE	24
3.7 Status of Test Condition Data Base	34
3.8 Status of 45 mm Bearing Thermal Model Investigation.	34
4.0 ANTICIPATED WORK.	49

SRS Technologies

LIST OF EXHIBITS

EXHIBIT NO.	PAGE
3.1	Highlights of the September, 1985 Reporting Period 6
3.1.1	Cage Torque Vs. Radial Clearance 7
3.1.2	Torque and Force Comparisons 10
3.2.1	Viscous Heat Generation Comparisons. 11
3.3.1	Bearing Component Temperatures 57mm Bearing 3000 lb. Axial Load 14
3.3.2	57mm Bearing Component Temperatures. 15
3.3.3	Percentage Increase in Component Temperature 3000 lb. Axial Load 16
3.3.4	Percentage Increase in Component Temperatures. 17
3.3.5	Temperature Vs. Load 18
3.3.6	Temperature Vs. Load 19
3.4.1	Relative Tangential Velocity Vs. Coolant Flow for BGR #4 - LOX Turbopump. 20
3.4.2	Axial Velocity Vs. Coolant Flow for BGR #4 LOX Turbopump . . . 22
3.4.3	Resultant Velocity Vs. Coolant Flow for BGR #4 - LOX Turbopump. 23
3.5.1	Contact Angle Vs. Radial Load - 57mm BGR 400 lb. Axial Load. . 25
3.5.2	Contact Angle Vs. Radial Load - 57mm BGR 1000 lb. Axial Load . 26
3.5.3	Contact Angle Vs. Radial Load - 57mm BGR 6000 lb. Axial Load . 27
3.5.4	Contact Angle Vs. Radial Load - 57mm BGR 12000 lb. Axial Load. 28
3.5.5	Track Width Vs. Radial Load - 57mm BGR 400 lb. Axial Load. . . 29
3.5.6	Track Width Vs. Radial Load - 57mm BGR 1000 lb. Axial Load . . 30
3.5.7	Track Width Vs. Radial Load - 57mm BGR 6000 lb. Axial Load . . 31
3.5.8	Track Width Vs. Radial Load - 57mm BGR 12000 lb. Axial Load. . 32
3.7.1	BSMT EUT Data Tapes. 35
3.8.1	Status of 45mm Bearing Thermal Model 36
3.8.2	45mm Bearing Heat Generation Summary 37
3.8.3	Parametric Analysis Variations 37
	APPENDIX A SAMPLE ADORE RUN. 40

SRS Technologies

1.0 SUMMARY

The magnitude and direction of fluid induced torques and forces on the 57 mm bearing cage is considered to be a contributing factor in possible cage instabilities that can produce intermittent high heating in the bearing. Analyses of the fluid forces and torques show that the resultant torques for the current configuration are in the direction to push or speed up the cage. A more stable condition is for the resultant torques to retard the cage. Modifications to the coolant flow diverter upstream of bearing #4 were defined that will provide resultant fluid torques in the stabilizing direction.

Heat generated by viscous fluid work has been estimated for two flow diverter configurations and a coolant flow of 10 lbs/sec to support the thermal evaluation of the LOX Bearing Materials Tester.

The analysis of the LOX turbopump turbine end bearing shows the sensitivity of bearing component temperatures to changes in coolant heat transfer coefficients and axial load. For loads greater than 5000 lbs and less than 6000 lbs, the bearing is thermally unstable and component temperatures increase until the bearing potentially fails.

Coolant velocities for the #4 LOX turbopump turbine end bearing have been estimated as a function of shaft speed and coolant flow rate. The results show that for the current flow rate of 4.6 lbs/sec, the coolant is pushing the balls and cage. An increase in flow of about 30% would cause the fluid to oppose the ball and cage motion. Flow fluctuations between these values could potentially provide an alternating force on the balls and cage contributing to cage instability.

Contact angles and track width data were developed for the 57 mm bearing as functions of shaft speed, and axial and radial loads. The axial loads ranged from 400 lbs to 1200 lbs, and the radial loads ranged from 100 to 5000 lbs.

The Advanced Dynamics of Rolling Elements (ADORE) computer program has been installed on the MSFC UNIVAC 1100 and a test case successfully run. Both the text output and the plotting output have been verified.

SRS Technologies

The Bearing Seal and Materials Tester - Test Condition Data Base has been developed. Averaging of currently available BSMT test data and entry of this average data into the data base has begun.

The parametric analysis of the operating characteristics of the LOX turbopump pump end bearing using the 45 mm bearing thermal model has begun. Initial results have revealed some numerical instabilities in the model which are currently being resolved.

SRS Technologies

2.0 SYNOPSIS OF PREVIOUS REPORTS

Previous reports included the items described below.

2.1 AUGUST, 1985

- o Cage Loads from Coolant Jets and Fluid Friction,
- o Viscous Heat Generation from Fluid Friction and Pumping,
- o Status of Test Condition Data Base, and
- o Status of 45 mm Bearing Investigation.

2.2 JULY, 1985

- o Status of LOX Turbopump Turbine End Bearing Thermal Investigation,
- o Status of Bearing Model Program ADORE,
- o Coolant Flow Diverter Velocities,
- o Status of Test Condition Data Base,
- o Status of 45 mm Bearing Thermal Model, and
- o Contact Angles and Ball Tracks as Function of Bearing Load.

2.3 JUNE, 1985

- o Status of LOX Turbopump Turbine End Bearing Thermal Investigation,
- o Status of Bearing Modeling Program ADORE,
- o Estimate of Ball to Cage Heat Generation,
- o Status of Test Condition Data Base, and
- o Status of 45 mm Bearing Thermal Model.

2.4 MAY, 1985

- o Status of LOX Turbopump Turbine end Bearing Investigation,
- o Status of Test Condition Data Base,
- o Status of 45 mm Bearing Thermal Model, and
- o Status of Bearing Modeling Program ADORE.

2.5 APRIL, 1985

- o Status of Test Condition Data Base,
- o Status of 45 mm Bearing Thermal Model, and

SRS Technologies

- o Investigation of the Sensitivity of Typical Heat Transfer Coefficients to Boundary Temperature and Pressure.

2.6 MARCH, 1985

- o Status of Test Condition Data Base,
- o Status of 45 mm Bearing Thermal Model,
- o SSME LOX Turbopump Bearing Coolant Flow Characteristics, and
- o Heat Generation for the 60 Hole Diverter.

2.7 FEBRUARY, 1985

- o Development of Test Condition Data Base,
- o LOX Tester Bearing Friction and Viscous Heat Estimates, and
- o Development of 45 mm Bearing Thermal Model.

2.8 JANUARY, 1985

- o Ball Excursions as a Function of Loading for 57 mm LOX Pump Bearing,
- o Cage Web Stresses for 57 mm LOX Pump Bearing,
- o LOX Turbopump 45 mm Bearing Parametric Data, and
- o Preliminary Requirements for Test Condition Data Base.

SRS Technologies

3.0 WORK PERFORMED DURING JULY - SEPTEMBER, 1985

This section describes the work performed during the three month period from July through September, 1985. Highlights of the September, 1985 effort are shown in Exhibit 3.1.

3.1 CAGE LOADS FROM COOLANT JETS AND FLUID FRICTION

The 57 mm LOX turbopump turbine end bearing cage (bearing #4) experiences forces from coolant jets impinging on the cage. These jets are produced by a coolant flow diverter plate that rotates at shaft speed and distributes the coolant through holes in the plate. These holes are angled downward 8° and swept back 51° to direct the jets between the cage and inner race, and to reduce the relative tangential velocity between the cage and fluid. Based on estimates reported in the March, 1985 progress report, the centrifugal forces produced by the high rotational speeds of the shaft are sufficient to bend the jets radially outward such that they impinge on the inner surface of the cage. The tangential component of these jets can act to speed up or slow down the cage depending on the direction of the relative tangential velocity component with respect to the cage. The relative velocity of the cage and tangential fluid component depends on cage speed, shaft speed, coolant flow rate and diverter geometry such as flow area and angles determining the direction of jet flow.

The current coolant flow diverter consists of 30 holes of 0.046" diameter angled radially inward 8° and swept back 51° . This configuration produces a moment on the cage, due to coolant jet impingement, in a direction to push or increase the cage rotational speed. The principal fluid force or moment in the direction to retard the cage rotation is the viscous drag of the fluid between the cage and outer race. This torque is a function of the clearance between the cage and outer race. Shown in Exhibit 3.1.1 is the cage driving and dragging torque estimated from these two sources.

These estimates are approximate and do not include dissipation of the jets due to surrounding fluid. As a first approximation the influence of velocity dissipation in the jet due to surrounding fluid can be made as follows¹. The characteristics of a typical jet discharging into a fluid are shown below.

¹Advanced Mechanics of Fluids; Hunter Rouse.

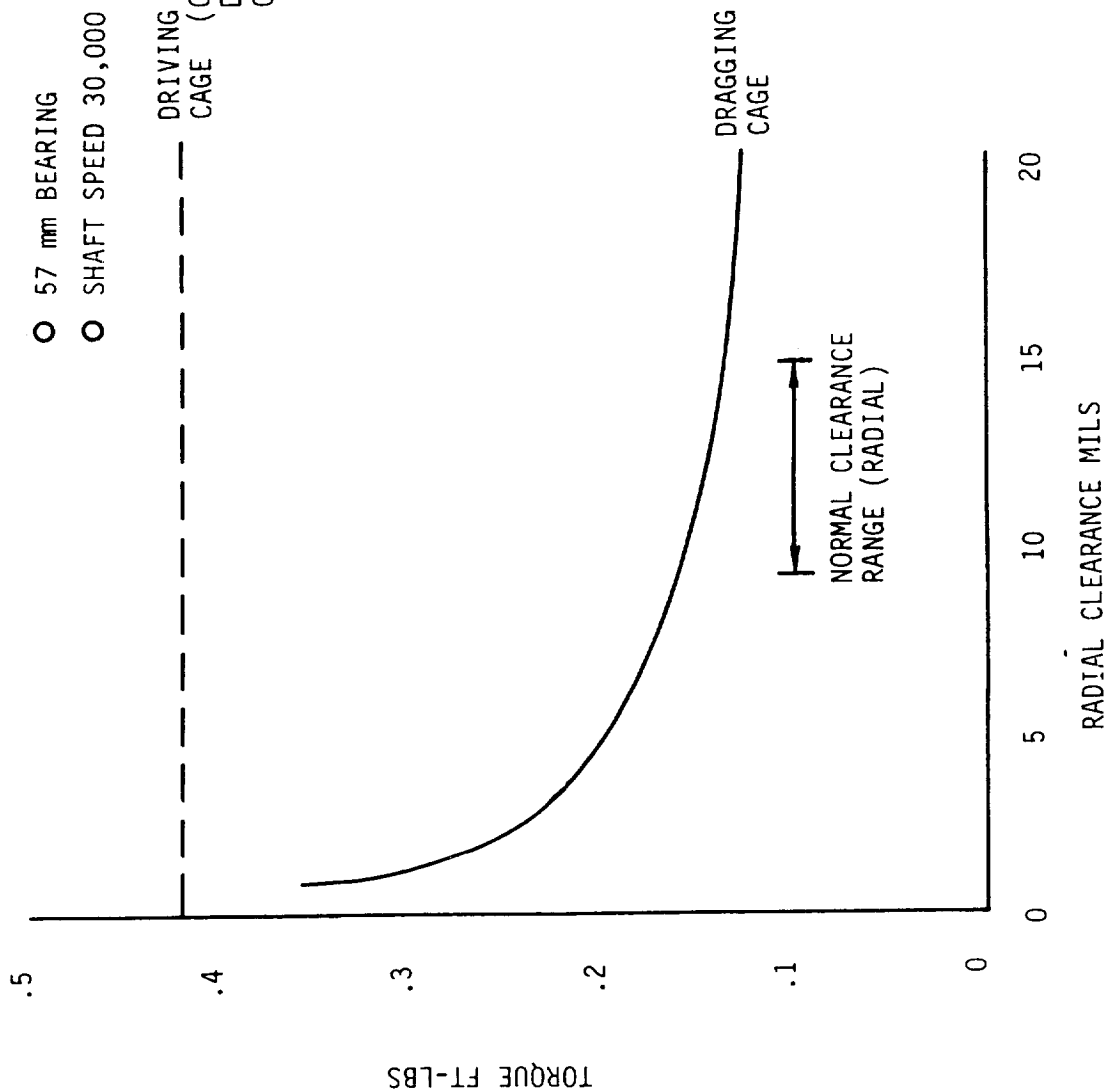
EXHIBIT 3.1

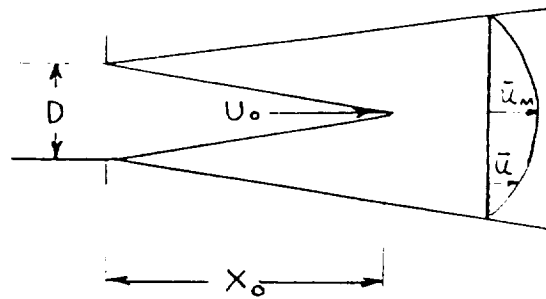
HIGHLIGHTS OF THE JULY - SEPTEMBER, 1985 REPORTING PERIOD

- 0 The ADORE bearing analysis program was operated successfully using the latest version of the Sperry UNIVAC FORTRAN optimizing compiler which improved the execution speed of the program. The problem with the plot output has been corrected.
- 0 All currently available BSMT test data tapes have been catalogued.
- 0 Parametric analysis of the SSME Turbopump Plume End Bearing using the 45mm bearing thermal model has begun. The initial results are being evaluated to determine the reliability of the thermal model.

EXHIBIT 3.1.1 CAGE TORQUE VS RADIAL CLEARANCE

- 57 mm BEARING
 - SHAFT SPEED 30,000 RPM
- DRIVING CAGE (CURRENT DIVERTER CONF.)





D = Orifice Diameter

U_0 = Exit Velocity

X_0 = Length of Irrotational Core

From Figure 127 of the reference:

$$\frac{X_0}{D} = 6.2$$

Therefore the length of the constant velocity zone for the 0.046" diameter orifice is: $X_0 = (6.2)(0.046) = 0.285"$. At the time of jet impingement on the cage, the distance travelled by the fluid is estimated to be 0.269 inches. Therefore, the irrotational core of the coolant jet impinges on the cage and very little velocity is dissipated over this distance, and the cage receives most of the available force in the jets.

The cage drag torque does not consider any direct contact between the cage and outer race. Coulomb friction due to these possible encounters is not considered. Even though not exact, these estimates are sufficient to identify characteristics that imply undesirable operating conditions for the bearing cage. As shown in Exhibit 3.1.1, the driving torque overcomes the dragging torque which is conducive to ball driven cage excitation which could lead to cage instability. A more stable condition would be for the fluid jets to cause a dragging torque on the cage allowing resultant fluid related torques to act against the direction of cage rotation.

This condition can be provided by minor modifications of the coolant diverter plate. By changing the hole angle from 51° to 60° and the hole size from 0.046 to 0.040, the torque produced from the impinging jets can be

SRS Technologies

changed from -0.42 to +0.6 ft-lbs. This provides a net torque of -0.283 ft lbs for the current configuration compared to +0.737 ft lbs for the modified diverter. These data are summarized in Exhibit 3.1.2. Also shown are the effects of increasing the flow rate with the current diverter geometry. Previous tests with this flow and diverter configuration resulted in cage delamination, attributed to the high jet impingement forces on the cage. As shown, the forces produced by the alternate configuration are about one third of the forces believed to have caused cage damage. Therefore, by the modifications previously described, the net fluid torque on the cage can be tailored to act in the direction to retard cage speed and provide a stabilizing effect on potential ball excited cage instability. This can be done while keeping the jet impingement forces well below those that have previously caused cage damage.

3.2 VISCOUS HEAT GENERATION FROM FLUID FRICTION AND PUMPING

Viscous heat generation from fluid stirring and pumping was estimated for the LOX Bearing and Seal Materials Tester (BSMT). Two diverter hole sizes were investigated: 0.046 inch and 0.062 inch diameter. Each diverter contained 60 holes, and the coolant flow was 10 lbs/sec per bearing pair for both LOX and LN_2 coolant. The results are shown in Exhibit 3.2.1. This information will be used for thermal modeling of the LOX BSMT.

3.3 LOX TURBOPUMP TURBINE END BEARING THERMAL INVESTIGATION

The 57 mm bearing thermal model developed for the BSMT was modified to simulate the SSME LOX turbopump turbine end flow conditions. For example, the coolant flow through the shaft and the diverter velocity effects specific to the pump were incorporated into the BSMT model. The model was run to determine the sensitivity of heat transfer coefficients on the average temperature of the bearing components. The vapor film coefficients were estimated for different assumed boundary layer temperature distributions and pressures. As discussed in the June, 1985 progress report, the high rotational speed of the bearing components could affect local coolant temperature and pressure. The 57 mm bearing model was run for the following conditions:

EXHIBIT 3.1.2. TORQUE AND FORCE COMPARISONS

1. Current Flow Diverter Configuration

- o Coolant Flow 4.6 lbs/sec
- o 30 Hole -.046" Diameter Holes
- o Hole Angle 51°

Source of Load	Torque (ft-lb)	Force (lbs)
o Cage/Outer Race	0.137	0.96
Fluid Friction (radial clearance 15 mils)		
o Coolant Jets	<u>-0.42*</u>	<u>-3.32</u>
TOTAL	-0.283	-2.36

2. Alternate Flow Diverter Configuration

- o Coolant Flow 4.6 lbs/sec
- o 30 Hole - .040" Diameter Holes
- o Hole Angle 60°

Source of Load	Torque (ft-lb)	Force (lbs)
o Cage/Outer Race	0.137	0.96
Fluid Friction (radial clearance 15 mils)		
o Coolant Jets	<u>0.6</u>	<u>4.69</u>
TOTAL	0.737	5.65

3. Current Flow Diverter Configuration

- o Coolant Flow 8 lbs/sec

Source of Load	Torque (ft-lb)	Force (lbs)
o Cage/Outer Race	0.137	0.96
Fluid Friction (radial clearance 15 mils)		
o Coolant Jets	<u>1.95</u>	<u>15.21</u>
TOTAL	2.087	16.17

* Negative Sign Means Torques and Forces are Pushing the Cage.

EXHIBIT 3.2.1. SUMMARY OF VISCOUS HEAT GENERATION (BTU/SEC)
COOLANT FLOW RATE OF 10 LBS/SEC FOR LOX & LN₂

60 hole diverter - .062" diameter holes - LOX

Component	Drive End		Load End	
	Brg 4	Brg 3	Brg 2	Brg 1
Balls (Spin & Drag)	13.35	2.07	2.07	13.35
Inner Race & Separator	1.1	1.1	1.1	1.1
Outer Race	3.2	3.2	3.2	3.2
Subtotal	17.65	6.37	6.37	17.65
Fluid Pumping and Diverter Holes	26.57		26.57	
Shaft: Hollow Section	6.58		1.76	
Subtotal	33.15		28.33	

60 hole diverter - .062" diameter holes - LN₂

Component	Drive End		Load End	
	Brg 4	Brg 3	Brg 2	Brg 1
Balls (Spin & Drag)	9.30	1.52	1.52	9.30
Inner Race & Separator	.81	.81	.81	.81
Outer Race	2.35	2.35	2.35	2.35
Subtotal	12.46	4.68	4.68	12.46
Fluid Pumping and Diverter Holes	30		30	
Shaft: Hollow Section	4.81		1.3	
Subtotal	34.81		31.3	

EXHIBIT 3.2.1. SUMMARY OF VISCOUS HEAT GENERATION (BTU/SEC)
COOLANT FLOW RATE OF 10 LBS/SEC FOR LOX & LN₂ (CON'T)

60 hole diverter - .046" diameter holes - LOX

Component	Drive End		Load End	
	Brg 4	Brg 3	Brg 2	Brg 1
Balls (Spin & Drag)	15.84	2.07	2.07	15.84
Inner Race & Separator	1.1	1.1	1.1	1.1
Outer Race	3.2	3.2	3.2	3.2
Subtotal	20.11	6.37	6.37	20.11
Fluid Pumping and Diverter Holes	33.49		33.49	
Shaft: Hollow Section	6.58		1.76	
Subtotal	40.07		35.25	

60 hole diverter - .046" diameter holes - LN₂

Component	Drive End		Load End	
	Brg 4	Brg 3	Brg 2	Brg 1
Balls (Spin & Drag)	26.05	1.52	1.52	26.05
Inner Race & Separator	.81	.81	.81	.81
Outer Race	2.35	2.35	2.35	2.35
Subtotal	29.21	4.68	4.68	29.21
Fluid Pumping and Diverter Holes	42.88		42.88	
Shaft: Hollow Section	4.81		1.3	
Subtotal	47.69		44.18	

SRS Technologies

- o Axial Loads (lbs) 3000, 4000, and 5,000
- o Local Coolant Pressure (psia) 250 and 300
- o Local Fluid Properties Evaluated at Film and Surface Temperatures
- o Coolant Flow Rate 4.6 lbs/sec
- o Coolant Inlet Temp = -240°F.

The results of the analysis are given in Exhibits 3.3.1 and 3.3.2 in terms of average component temperatures and maximum temperatures in the bearing tracks. These data were used to determine the percentage change in temperature for the various conditions as shown in Exhibits 3.3.3 and 3.3.4. At the higher loads, the component average temperatures appear to be more sensitive to variations in heat transfer coefficients especially the inner and outer races. Exhibit 3.3.5 shows the component average and track temperatures as a function of axial load for a coolant pressure of 300 psia. Exhibit 3.3.6 shows similar information for a coolant pressure of 250 psia. A 6000 lb axial load condition was attempted but the solution failed to converge indicating a thermally unstable condition. This agrees with the increasing slope of the temperature curves as the load is increased.

3.4 COOLANT FLOW DIVERTER VELOCITIES

The Space Shuttle Main Engine (SSME) liquid oxygen (LOX) turbopump turbine end bearing coolant flow circuit includes a flow diverter plate upstream of the Number 4 bearing. The purpose of the diverter is to provide coolant directly to the bearing components (balls and inner race), and reduce the relative velocities between the coolant and the bearing balls and cage. The magnitude and direction of these velocities are dependent on diverter geometry, coolant flow, and shaft speed. The current diverter is a circular plate consisting of 30 - 0.046" diameter holes, angled 39° from a tangent to the outer circumference to the plate. The angle serves to reduce the relative tangential velocity between the coolant and bearing balls and cage.

An analysis was done to evaluate the coolant velocities as a function of coolant flow and shaft speed. Shown in Exhibit 3.4.1 is the relative tangential velocity between the coolant and balls as a function of shaft speed and coolant flow. The diverter is rotating at shaft speed which is about 55% greater than ball or cage speed. The axial velocity of the coolant jets increases with coolant flow and since they are angled back, the net result is

EXHIBIT 3.3.1. BEARING COMPONENT TEMPERATURES 57mm BEARING 3000 LB AXIAL LOAD

CONDITION	COMPONENT	TEMPERATURE OF	
		AVERAGE	MAX TRACK
o 300 PSIA o FILM TEMP	BALL	167	448
	INNER RACE	-136	325
	OUTER RACE	-115	146
o 300 PSIA o WALL TEMP	BALL	223	546
	INNER RACE	-110	378
	OUTER RACE	-100	184
o 250 PSIA o FILM TEMP	BALL	219	539
	INNER RACE	-108	371
	OUTER RACE	-107	166
o 250 PSIA o WALL TEMP	BALL	273	596
	INNER RACE	-90	424
	OUTER RACE	-91	203

EXHIBIT 3.3.2. 57mm BEARING COMPONENT TEMPERATURES

CONDITIONS (HEAT TRANSFER PROPERTIES EVALUATED AT FILM TEMP.)	COMPONENT	TEMPERATURE (°F)		
		AVERAGE	MAX TRACK	
<ul style="list-style-type: none"> o 4000lb AXIAL LOAD o 300 PSIA 	BALL	352.	772.	
	INNER RACE	-61.	562.	
	OUTER RACE	12.	349.	
<ul style="list-style-type: none"> o 4000lb AXIAL LOAD o 250 PSIA 	BALL	430.	847.	
	INNER RACE	-31.	625	
	OUTER	31.	380	
<ul style="list-style-type: none"> o 5000lb AXIAL LOAD o 300 PSIA 	BALL	624.	1205.	
	INNER RACE	13.	859.	
	OUTER RACE	160.	629.	
<ul style="list-style-type: none"> o 5000lb AXIAL LOAD o 250 PSIA 	BALL	867	1508	
	INNER RACE	135	1082	
	OUTER RACE	285	815	

EXHIBIT 3.3.3. PERCENTAGE INCREASE IN COMPONENT TEMPERATURE
3000 LB AXIAL LOAD

CONDITION	COMPONENT	% INCREASE IN TEMP	
		AVERAGE	MAX TRACK
o 300 PSIA o FILM TO WALL COMPARISON	BALL	33	12
	INNER RACE	18	16
	OUTER RACE	13	26
o 250 PSIA o FILM TO WALL COMPARISON	BALL	25	11
	INNER RACE	17	14
	OUTER RACE	16	22
o FILM 300 TO 250 COMPARISON	BALL	31	10
	INNER RACE	20	14
	OUTER RACE	7	13
o WALL 300 TO 250 COMPARISON	BALL	22	9
	INNER RACE	18	12
	OUTER RACE	9	11

EXHIBIT 3.3.4 - PERCENTAGE INCREASE IN COMPONENT TEMPERATURE

CONDITIONS (HEAT TRANSFER PROPERTIES EVALUATED FILM TEMP)	COMPONENT	% INCREASE IN TEMP(°F)	
		AVERAGE	MAX TRACK
o 4000lb AXIAL LOAD o 300 TO 250 PSIA COMPARISON	BALL	22	10
	INNER RACE	49	11
	OUTER RACE	158	9
o 5000lb AXIAL LOAD o 300 TO 250 PSIA COMPARISON	BALL	40	25
	INNER RACE	938	26
	OUTER RACE	78	30

EXHIBIT 3.3.5 - TEMPERATURE VS. LOAD

- o 57 mm BEARING
- o SHAFT SPEED 30,000 RPM
- o COOLANT FLOW & PRESSURE
(4.6 LBS/SEC 300 PSIA)
- o HEAT TRANSFER PROPERTIES
EVALUATED @ FILM TEMP.

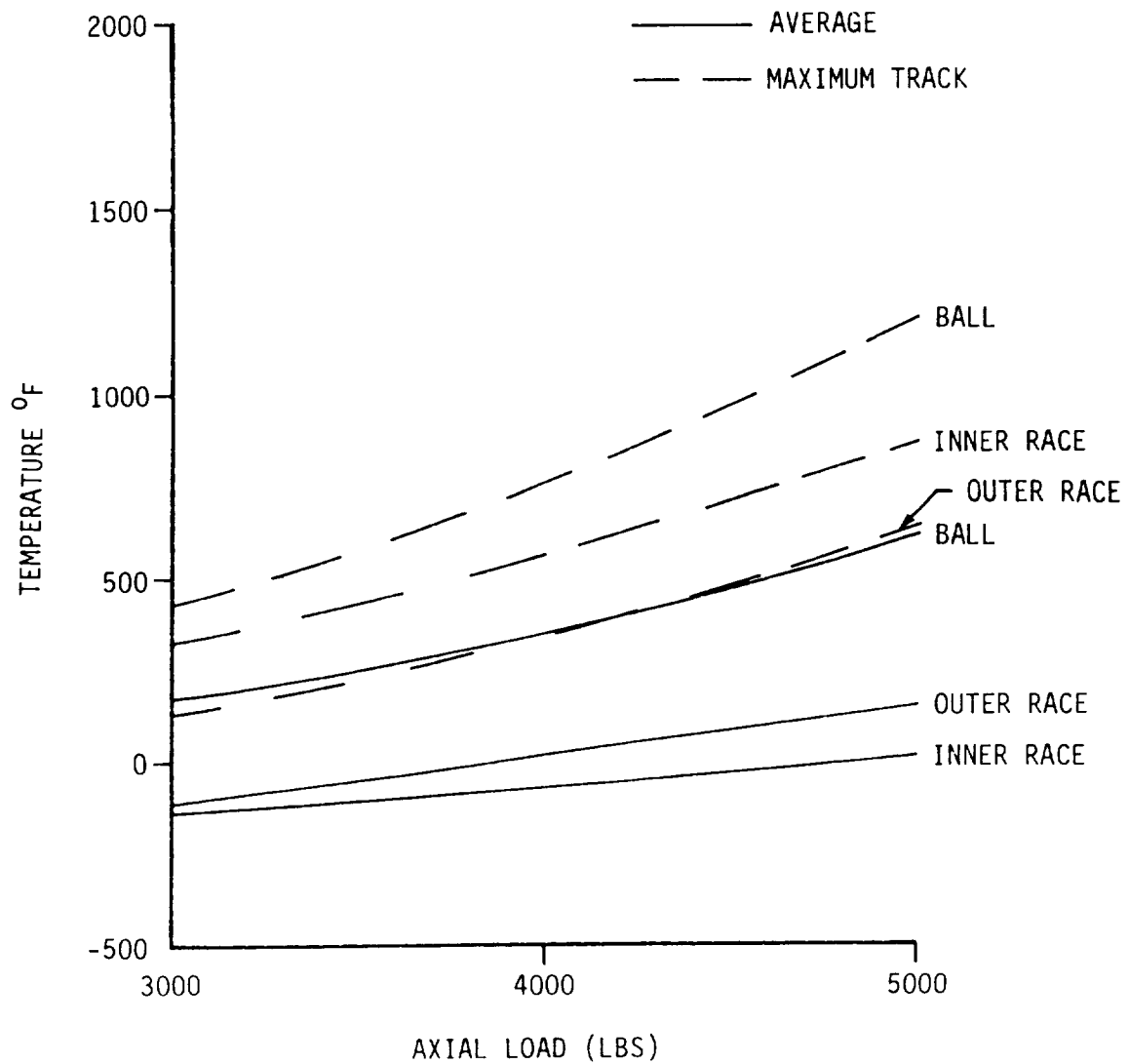


EXHIBIT 3.3.6 - TEMPERATURE VS. LOAD

- o 57 mm BEARING
- o SHAFT SPEED 30,000 RPM
- o COOLANT FLOW & PRESSURE
4.6 LBS/SEC 250 PSIA
- o HEAT TRANSFER PROPERTIES
EVALUATED @ FILM TEMPERATURE

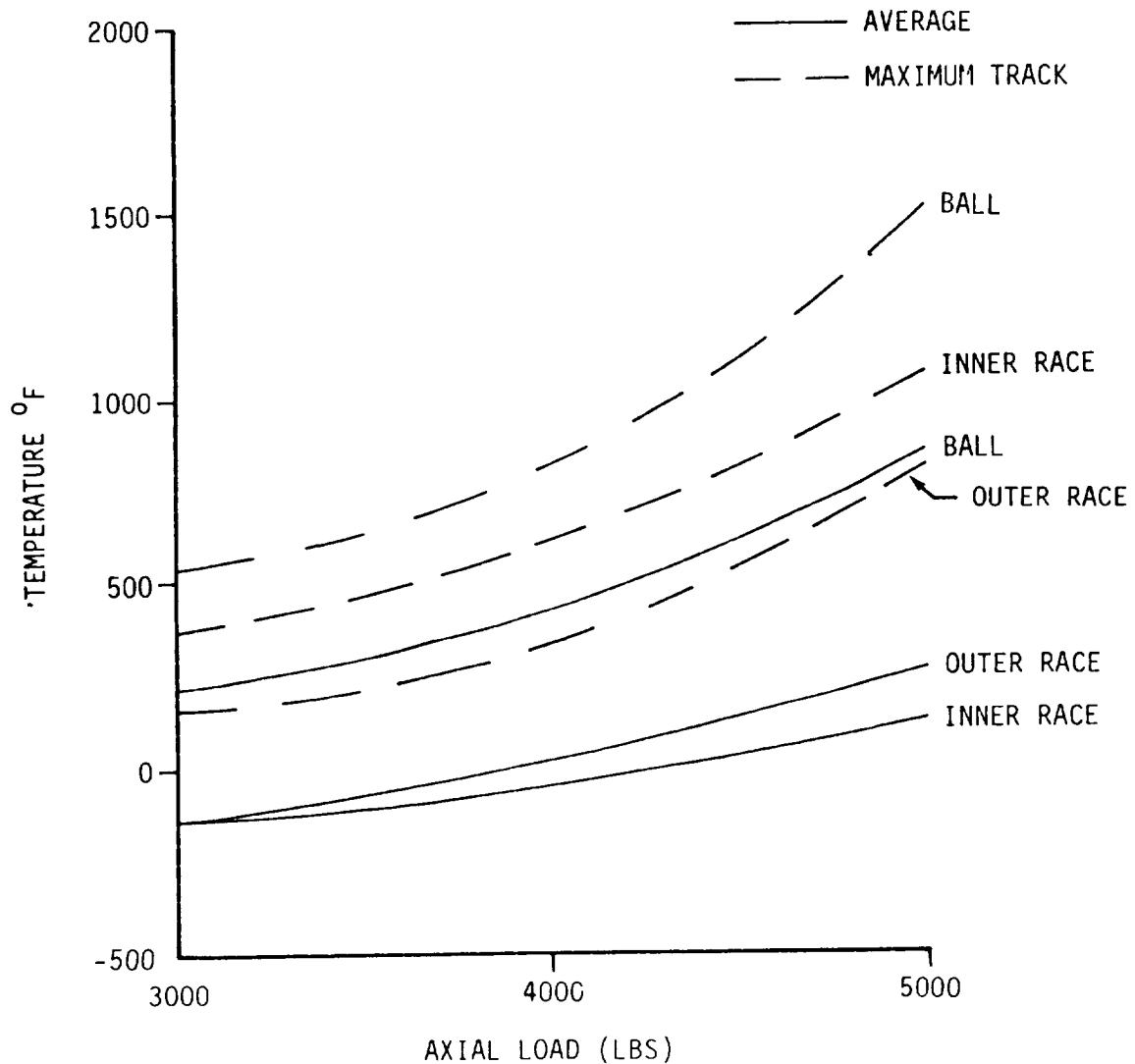
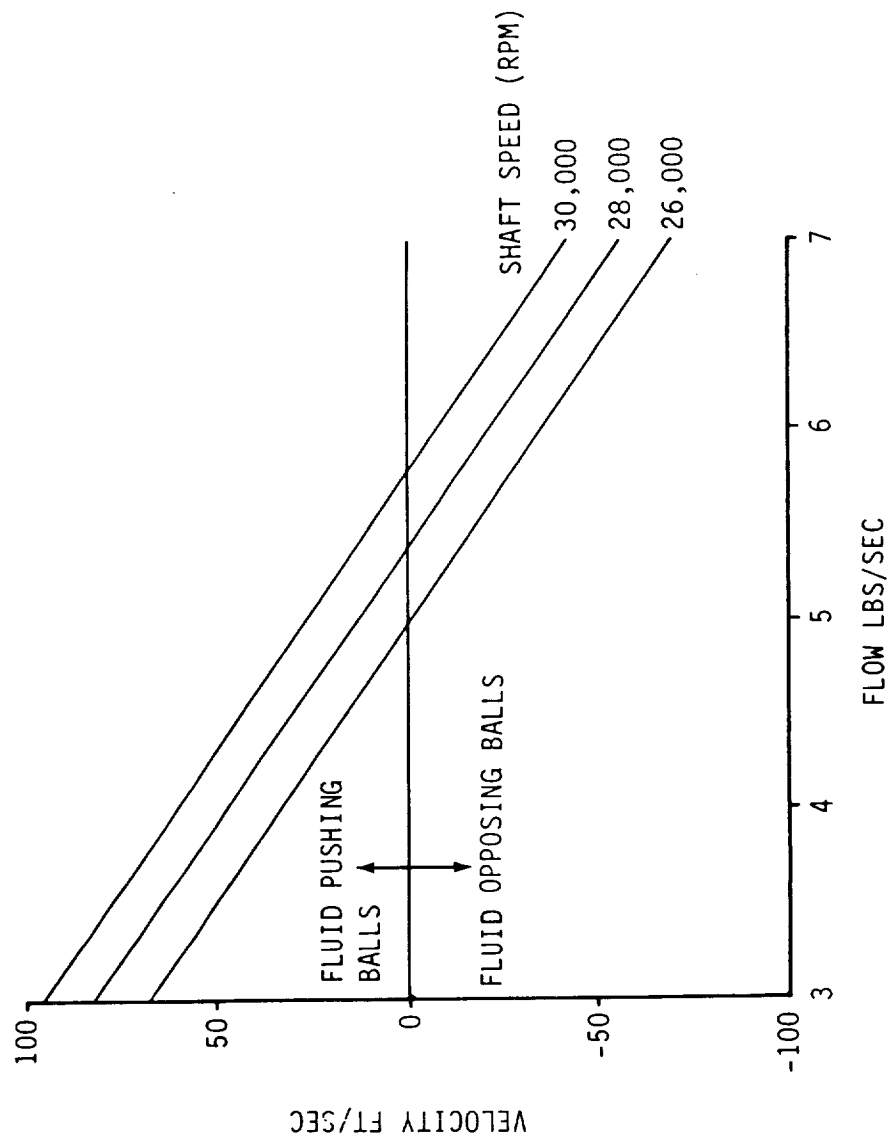


EXHIBIT 3.4.1.
RELATIVE TANGENTIAL VELOCITY VS COOLANT FLOW FOR BGR #4 - LOX TURBO PUMP

30 - .046" DIAMETER HOLE
FLOW DIVERTER - LOX COOLANT



SRS Technologies

to reduce the relative tangential velocity between the bearing balls and coolant. The tangential velocity of the coolant increases with shaft speed and as flow rate increases the fluid tends to oppose rather than push the balls as shown in Exhibit 3.4.1.

Since the nominal coolant flow rate is about 4.6 lbs/sec for the LOX turbopump turbine end bearings, the coolant tries to speed up the balls and cage for this condition. In addition, the current flow rate is fairly close to flows that would make the relative tangential velocity zero. For example, a 30% increase in flow would provide 6 lbs/sec which would cause the flow to slightly oppose the ball speed. Slight variations in flow around the velocity zero point could cause an alternating tangential force on the balls and cage which could contribute to a forcing function possibly causing cage instability.

Exhibit 3.4.2 provides the axial component of the coolant velocity as a function of coolant flow. Since this component is parallel to the bearing axis, it is independent of shaft speed.

The resultant velocity of the coolant impinging on the bearing balls and cage is shown in Exhibit 3.4.3 as a function of coolant flow and shaft speed. As indicated, the relative tangential velocity increases in the negative direction, for higher flow rates, as the shaft speed decreases. Since the resultant velocity is the vector sum of the axial and relative tangential velocities, this causes the curves shown in Exhibit 3.4.3 to cross as the flow rate increases. The coolant flow that minimizes the resultant velocity can be expressed as:

$$w = \rho A \omega [r_h - .45 r_p] \cos \theta$$

where w = Coolant flow

A = Coolant flow area

ω = Shaft speed

r_h = Radius to coolant holes

r_p = Pitch radius

θ = Hole back angle.

The flow rates that minimize the resultant coolant velocities are noted on Exhibit 3.4.3. The above expression can also be used to select the

EXHIBIT 3.4.2.
AXIAL VELOCITY VS COOLANT FLOW FOR BGR #4 - LOX TURBO PUMP

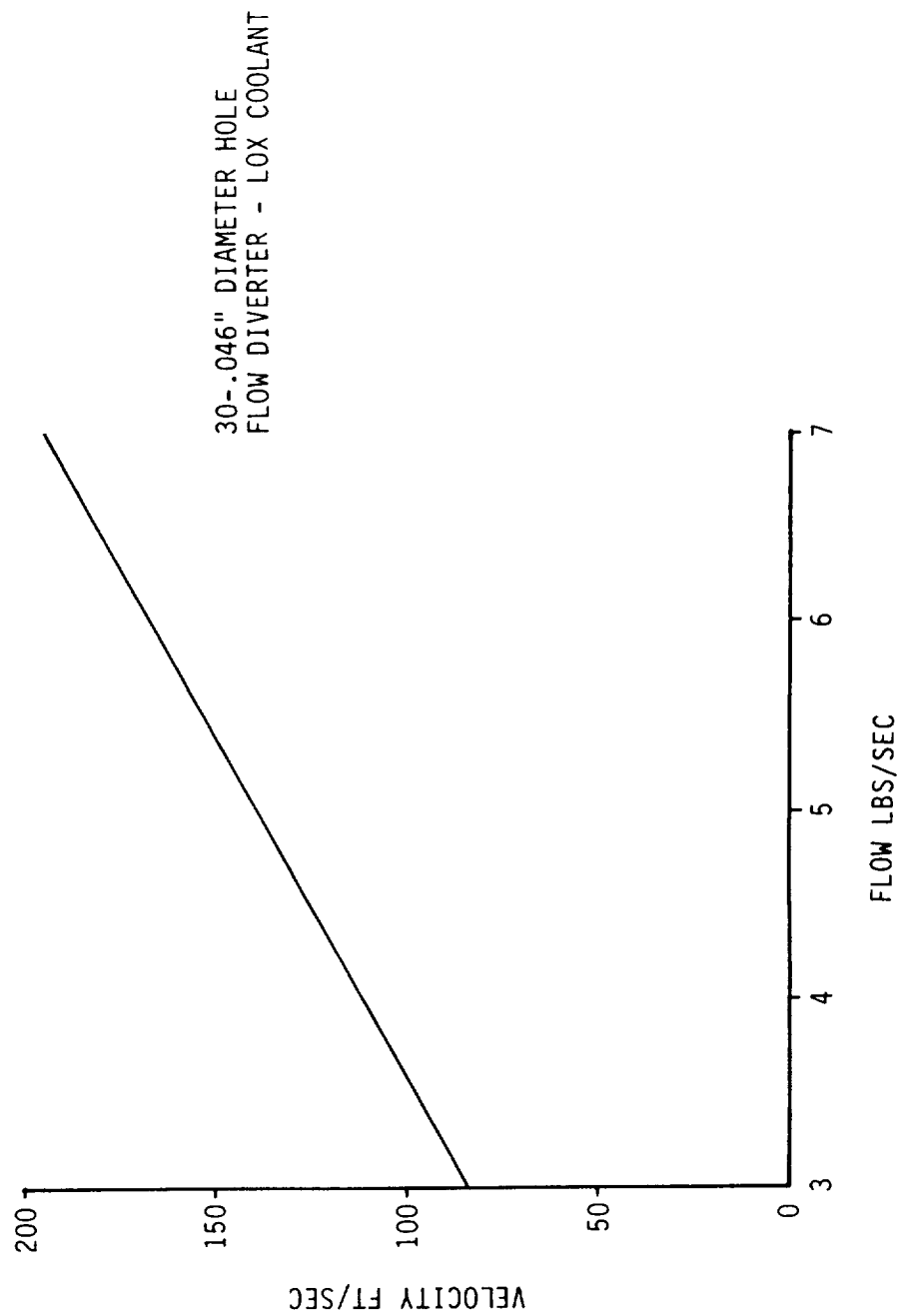
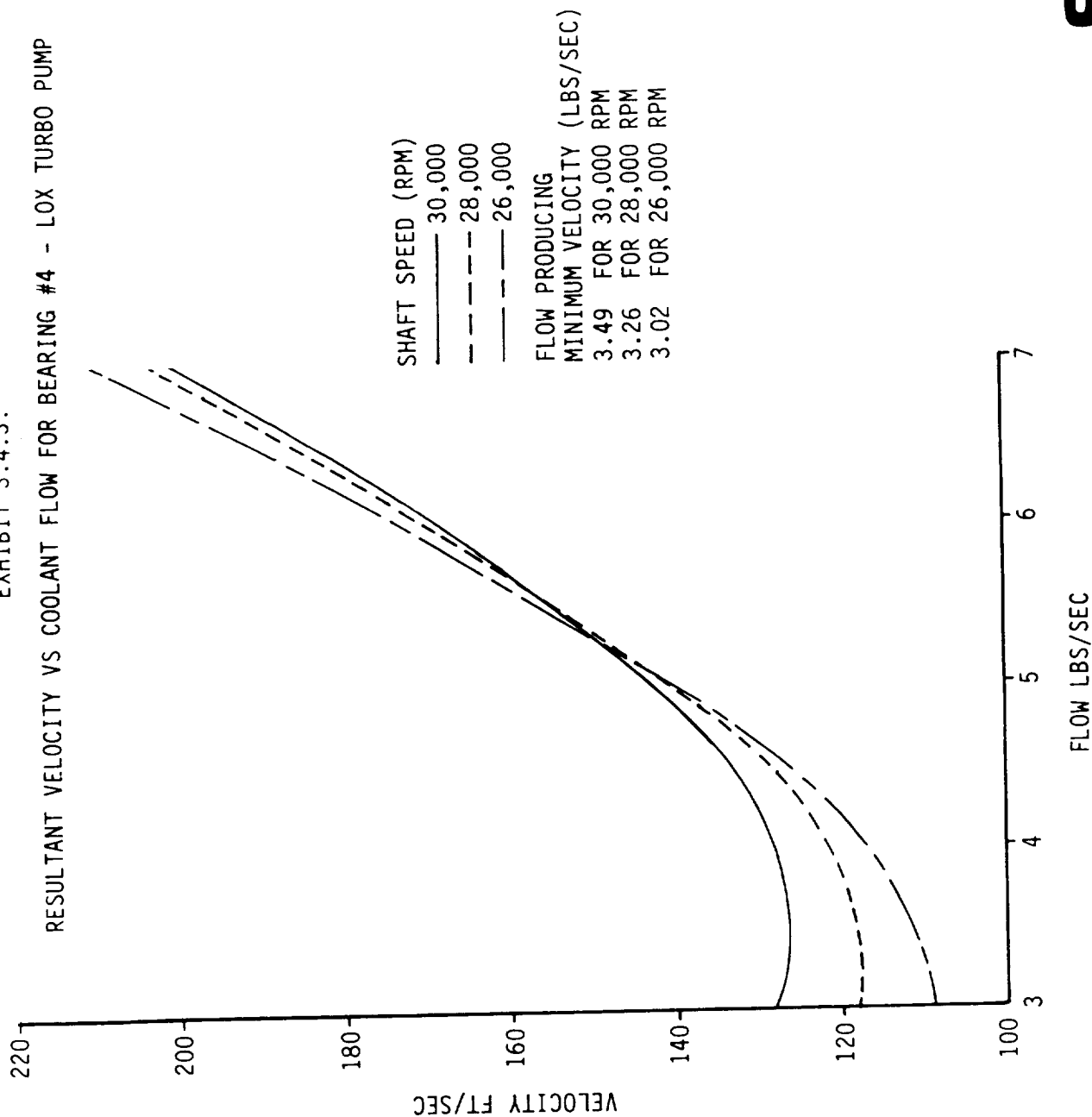


EXHIBIT 3.4.3.

RESULTANT VELOCITY VS COOLANT FLOW FOR BEARING #4 - LOX TURBO PUMP



SRS Technologies

diverter geometry that will minimize the resultant coolant velocity for given coolant flow rates and shaft speeds. For example the equation can be rearranged to give:

$$A \cos \theta = \frac{w}{\rho \omega [r_h - .45r_p]}$$

This provides a choice of flow areas and diverter hole angles that provide a minimum resultant coolant velocity for a specified coolant flow rate and shaft speed.

3.5 CONTACT ANGLES AND BALL TRACKS AS FUNCTION OF BEARING LOAD

The 57 mm turbine end LOX turbopump bearing model was used to provide parametric information on the effects of shaft speed and axial and radial loads on operating contact angles and inner race ball tracks. The axial loads ranged from 400 to 12000 lbs and the radial loads were from 100 to 5000 lbs. The contact angle data are provided in Exhibits 3.5.1 through 3.5.4, and the inner race track width data are provided in Exhibits 3.5.5 through 3.5.8. The track width data provides the width of the track caused by the ball excursions due to the azimuth change in contact angle as the ball rotates around the inner race. Since the track width data shown does not include the width of the contact area, the actual wear track should be wider by the length of the major axis of the contact ellipse. For the cases shown, the load is applied at an azimuth angle of 180° and the bearing reaction occurs at an azimuth angle of zero degrees. Since each ball has a different contact angle, only the two extremes were plotted.

3.6 STATUS OF BEARING MODELING PROGRAM ADORE

The ADORE (Advanced Dynamics of Rolling Elements) bearing analysis program is now fully operational on the MSFC UNIVAC 1100 computer system. This section outlines the major problems that were overcome to install the program on the UNIVAC during the last quarter.

A new Sperry UNIVAC FORTRAN compiler was installed at MSFC during the last month. This new version corrected the problem in its code 'optimizer' feature. The optimizer analyzes the FORTRAN source code and rewrites it to

EXHIBIT 3.5.1.
CONTACT ANGLES VS. RADIAL LOAD - 57mm BEARING

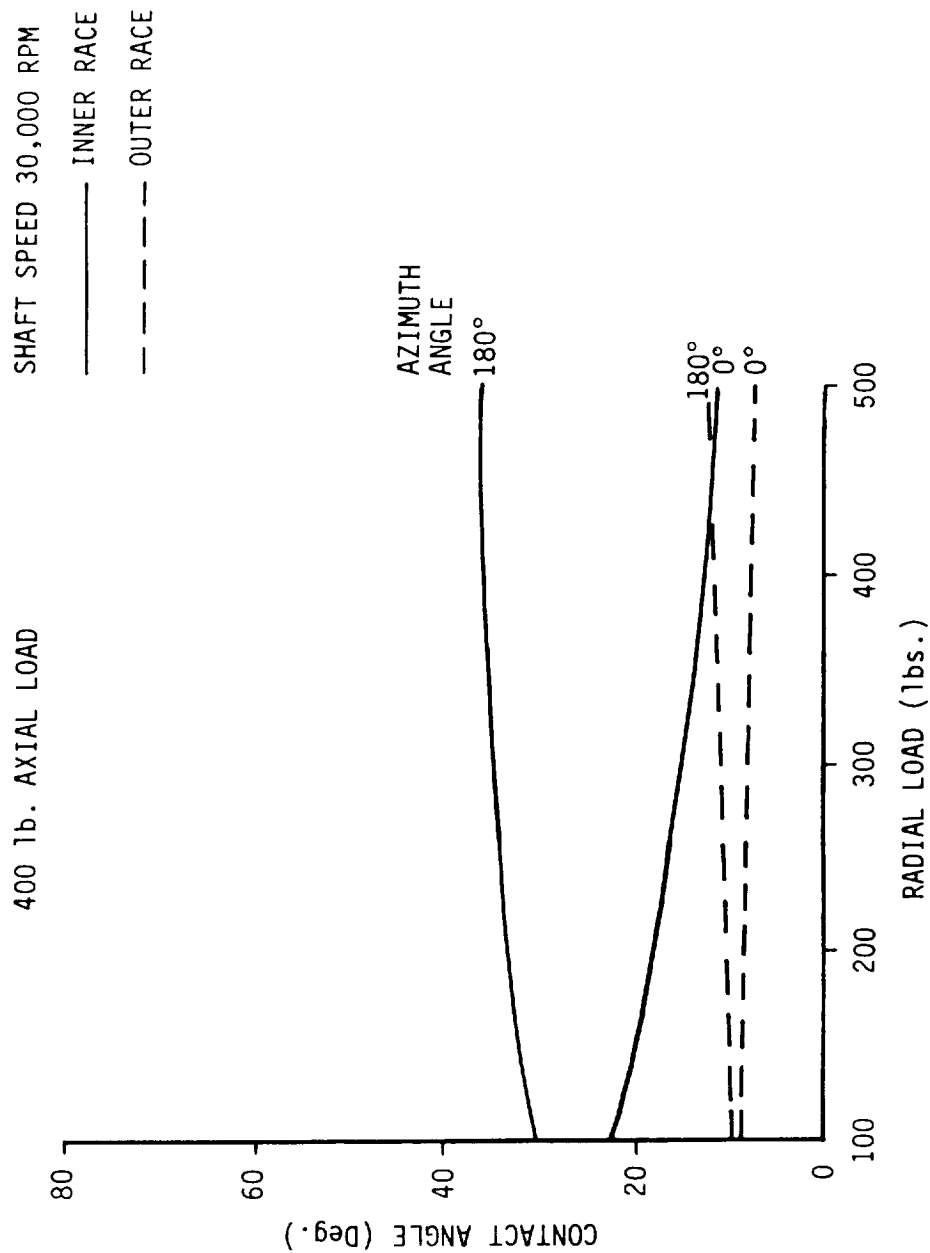


EXHIBIT 3.5.2.

CONTACT ANGLE VS. RADIAL LOAD - 57mm BEARING

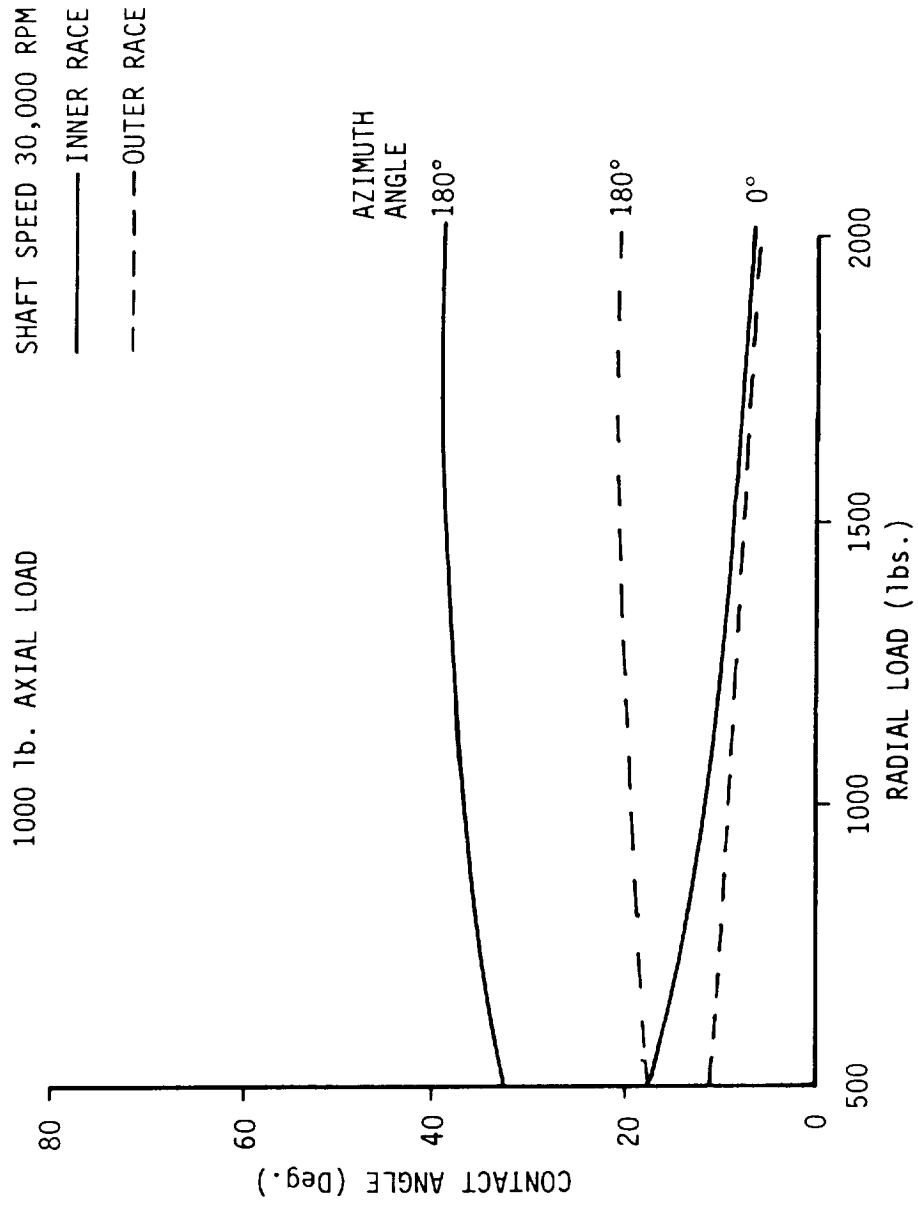


EXHIBIT 3.5.3. CONTACT ANGLE VS. RADIAL LOAD

6000 lb. AXIAL LOAD SHAFT SPEED 30,000 RPM

—— INNER RACE

--- OUTER RACE

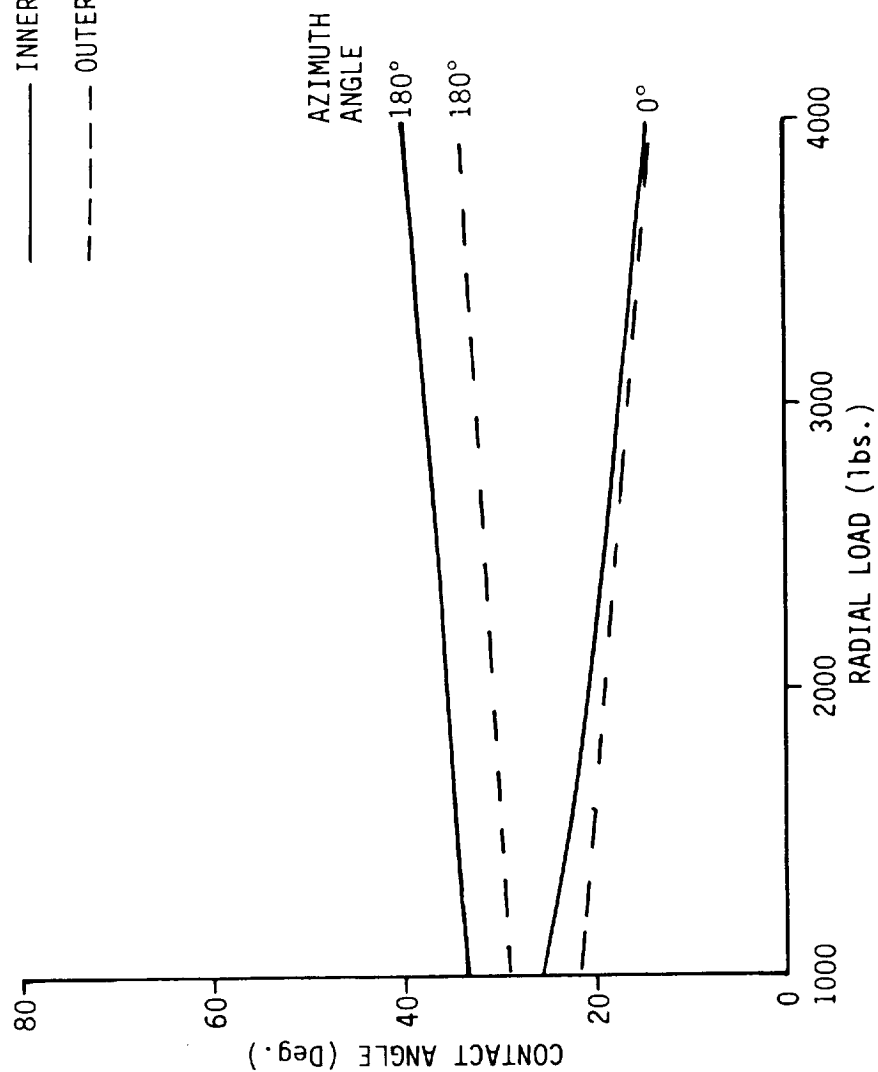


EXHIBIT 3.5.4.

CONTACT ANGLE VS. RADIAL LOAD -- 57mm BEARING

12,000 lb. AXIAL LOAD SHAFT SPEED 30,000 RPM

—— INNER RACE
 - - - - - OUTER RACE

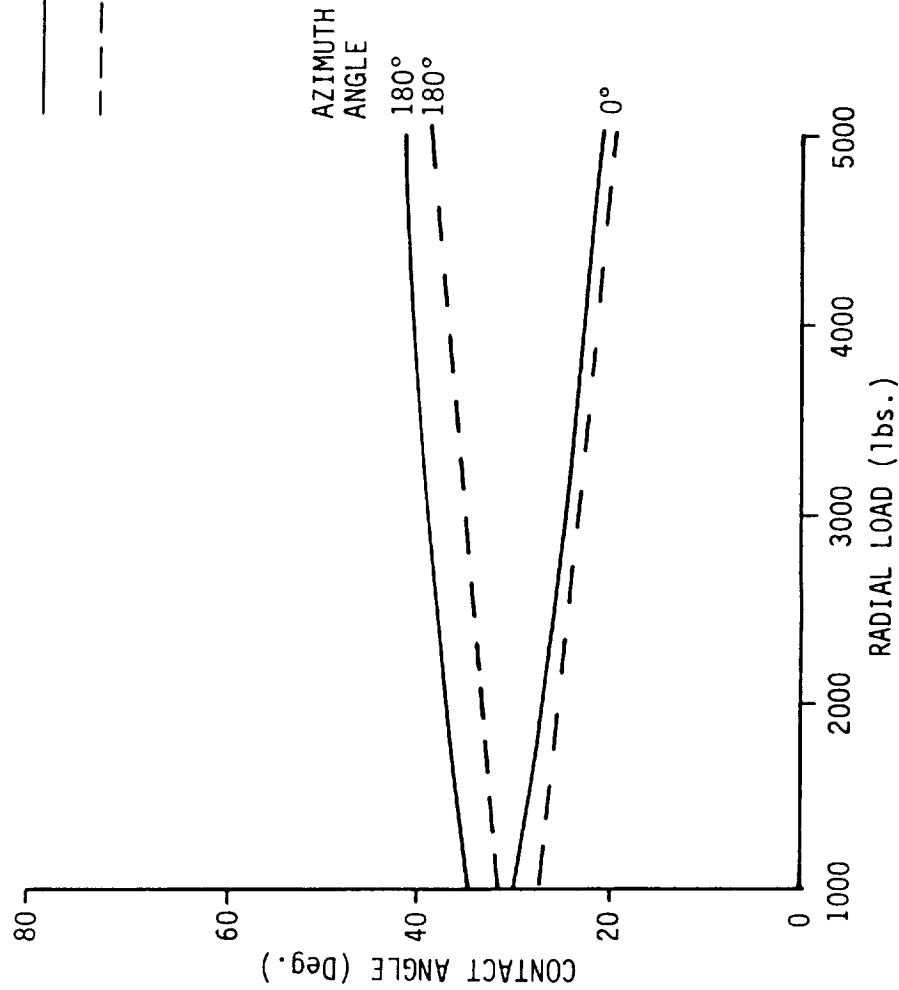


EXHIBIT 3.5.5.

TRACK WIDTH VS. RADIAL LOAD - 57mm BEARING

400 lb. AXIAL LOAD SHAFT SPEED 30,000 RPM

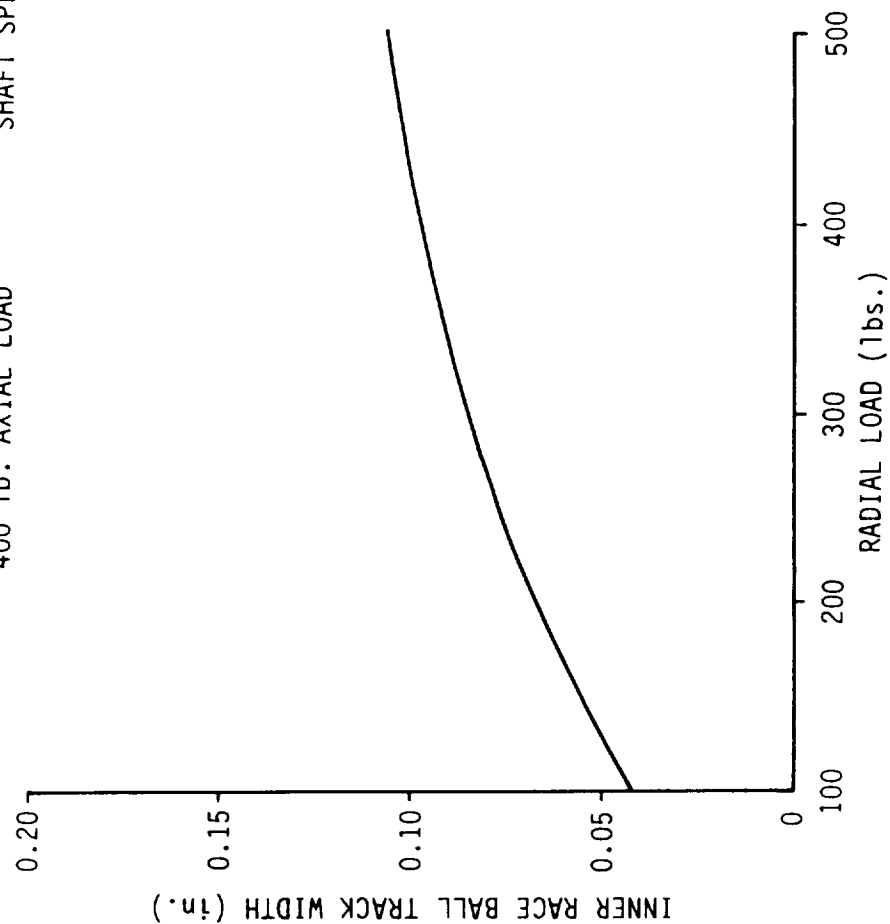


EXHIBIT 3.5.6. TRACK WIDTH VS. RADIAL LOAD - 57mm BEARING

1000 lb. AXIAL LOAD SHAFT SPEED 30,000 RPM

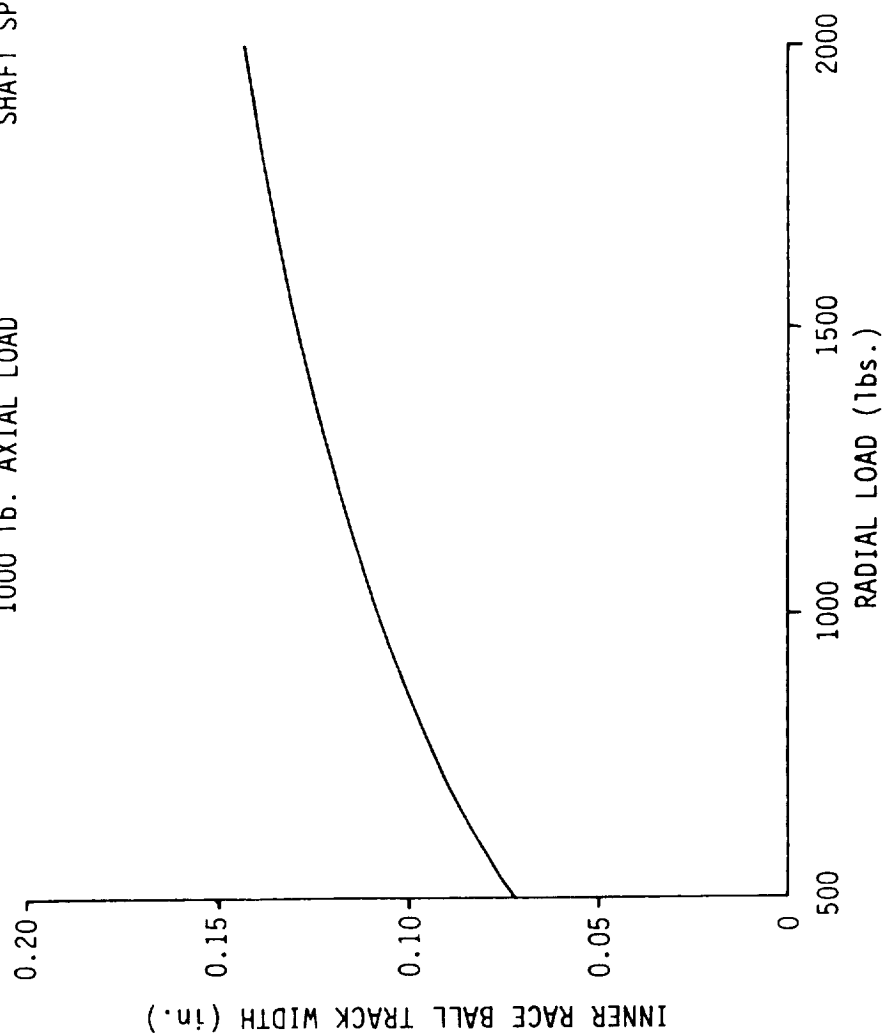


EXHIBIT 3.5.7.

TRACK WIDTH VS. RADIAL LOAD - 57mm BEARING

6000 lb. AXIAL LOAD SHAFT SPEED 30,000 RPM

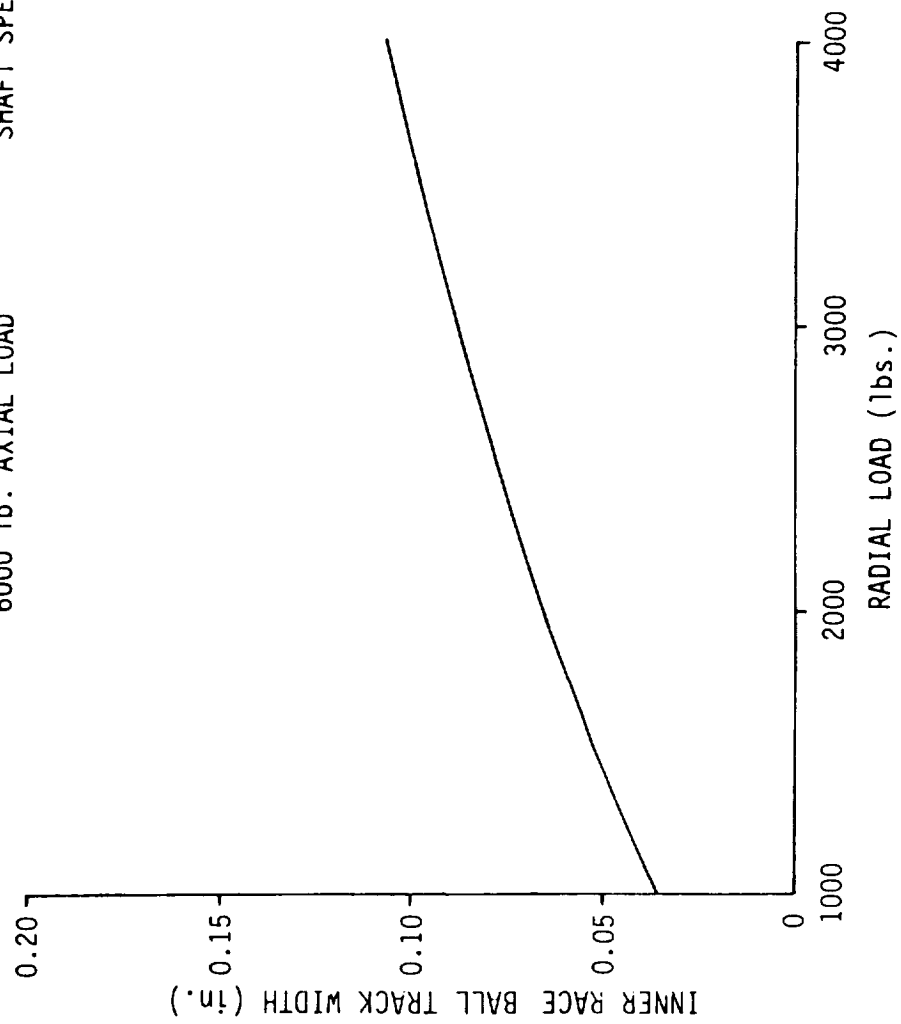
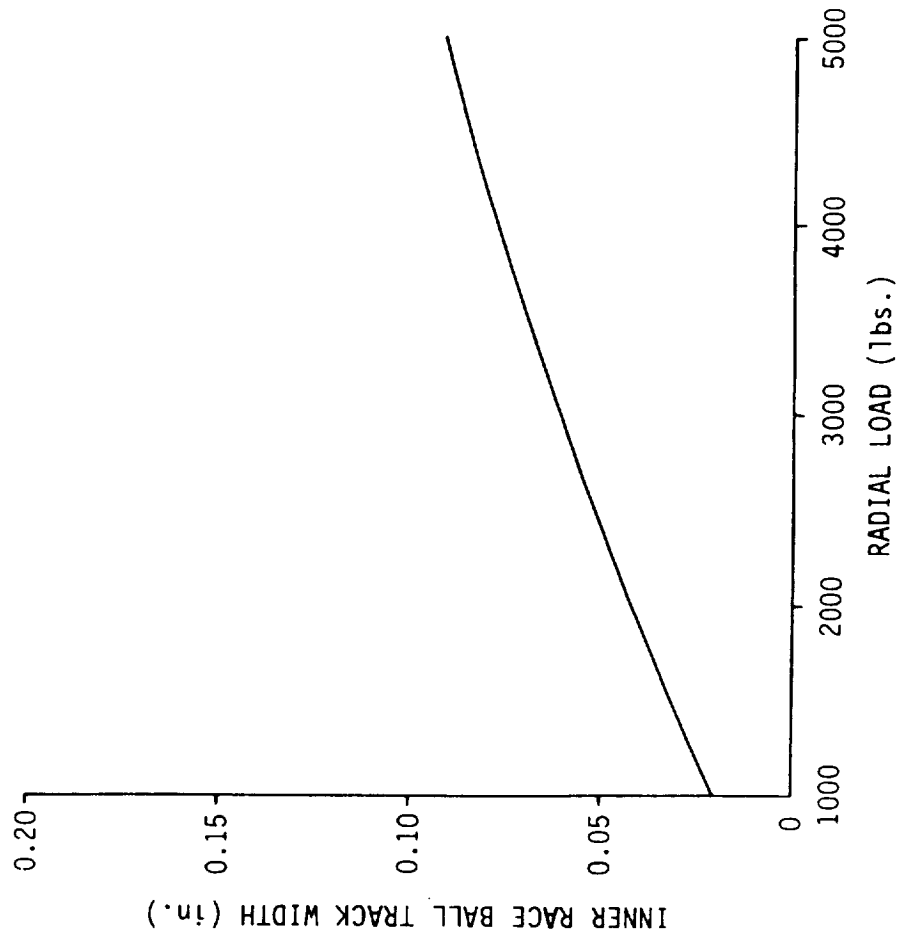


EXHIBIT 3.5.8.

TRACK WIDTH VS. RADIAL LOAD - 57mm BEARING

12,000 lb. AXIAL LOAD SHAFT SPEED 30,000 RPM



SRS Technologies

produce a more efficient program that runs faster than non-optimized code. Because of its lengthy computations, ADORE needs to be optimized to increase its execution speed. However, the optimizer portion of the previous Sperry FORTRAN compiler contained an error that was triggered by the ADORE code, resulting in an executable program that contained errors not present in the original source code. ADORE was used as a test case for the new compiler version and the current optimized version of ADORE runs successfully.

A major feature of the ADORE program is its plotted output. This portion of the program was also successfully installed September, 1985. One problem with this section of code was a conflict between data files. Both ADORE and the DISSPLA graphics routines were trying to use the same data file which caused an error termination of the program. FORTRAN data files are represented internally by "logical unit numbers" and both ADORE AND DISSPLA were trying to use No. 17. The conflict was resolved by changing the unit number used by ADORE from 17 to 19. Another problem surfaced when the ADORE plot routine (ADRP1) was trying to read an empty data file. During an ADORE run, the plot output can be saved for a maximum of six elements (an element can be either a rolling element, cage segments, inner race, or outer race). These plot outputs are saved in up to six files labeled SOL1 through SOL6. When the plot portion of ADORE is executed, an attempt is made to read each file. If a file is empty because less than six elements were chosen to plot then the program terminates in error. After a discussion with Dr. Gupta, the program's author, a method was derived to save the number of elements chosen to be plotted as a variable and to pass it as an argument to the plot routine ADRP1. This allows ADRP1 to know how many files are available and it will not attempt to read an empty file.

Once the plot portion of ADORE has run, the DISSPLA graphics post processor can be used to either show the plots on the terminal screen where they can be copied by local electrostatic hard copy units, or the plots can be sent to the MSFC FR80 micrographics system. This system will take the plots and photograph them onto microfiche, from which 8 1/2 x 11 copies can be made. While the resolution is comparable to the local hard copy plots, the microfiche can be easily archived.

SRS Technologies

Appendix A shows a sample ADORE run produced on the UNIVAC 1100/80 system. The first part shows the printed output for a 10 time step version of a sample case presented in the ADORE User's Manual. The second section shows a series of plots produced for a 5 time step version of the same model. Only a few of the plots were included here to illustrate the capability. These plots were produced from microfiche using the FR80 micrographics system.

3.7 STATUS OF TEST CONDITION DATA BASE

During this reporting period, substantial progress was made on the development of the Test Condition Data Base system. As outlined in earlier reports, this system consists of two main programs - one that will access BSMT data from the EUT tapes and compute average data values over a given time segment, and a data base software system on which to store and retrieve this averaged test data. Both programs are now operational. Previously, significant problems were encountered on the UNIVAC 1100 system when attempting to use the ACCESS data retrieval subroutine to get the data from the data base files. These problems were solved and the software was successfully used to average data from a recent non-rotational test (no. 201N0101*NR). The program currently computes the population standard deviation of the sample during the given time segment.

Subsequent to the completion of the Test Condition Data Base System averaging of the available rotational test data and its entry into the data base was initiated. The available test data was being stored by Boeing Computer Services. These tapes were collected and reviewed. Exhibit 3.7.1 is a list of these tapes, their dates, and any comments found on the tape labels. These tapes are all in EUT (Engineering Units Tape) format. To be plotted or averaged, these tapes must be converted to a file format used by the PLOT programs that display the data. Methods for these conversions and provisions for long-term storage of the EUT tapes will be examined during the next reporting period.

3.8 STATUS OF 45 MM BEARING INVESTIGATION

During this quarter, the bearing thermal model for the SSME 45 mm turbopump bearing (pump end) has been completed. A summary of the work

EXHIBIT 3.7.1 BSMT DATA TAPES

	Tape Label	Date of Test	Comments
1	202N0101-NR	Aug 8, 1985	
2	201N1001-R	Aug 8, 1984	
3	201N0801-R	Jul 12, 1984	
4	201N0701-R1	Jun 22, 1984	
5	201N0601-R	Jun 8, 1984	12:43 - 12:44
6	201N0601-R	Jun 8, 1984	10:44 - 12:40
7	201N0601-R	Jun 8, 1984	12:40 - 12:43
8	201N0601-R1	Jun 8, 1984	12:44 - 12:49
9	201N0501-R2	May 15, 1984	12:26 - 12:33
10	201N0407-R	Mar 30, 1984	15:27 - 15:29
11	201N0406-R1	Mar 9, 1984	
12	201N0406-R	Mar 9, 1984	
13	201N0406-R2	Mar 9, 1984	15:25 - 15:31
14	201N0404-R	Feb 23, 1984	
15	201N03-NR	Dec 1, 1983	
16	201N01-NR	Dec 1, 1983	11:25 - 12:37
17	201N03-NR	Nov 30, 1983	
18	201N03-NR	Nov 22, 1983	
19	201N03-NR	Nov 16, 1983	
20	201N03-NR1	Nov 16, 1983	12:35 - 12:38
21	P051-PC-5	Oct 21, 1983	
22	P051-PC-6	Oct 3, 1983	
23	P051-PC600	Sep 28, 1983	DAY 271
24	P051-PC-4	Sep 21, 1983	
25	P051-PC-4	Sep 21, 1983	14:29 - 14:55
26	P051-PC-3	Sep 20, 1983	12:39 - 14:15
27	P051-PC-3	Sep 20, 1983	
28	104L08-R	Jun 18, 1982	
29	500TCP003E*BMT3	Mar 24, 1982	
30	500TCP003A*BMT4	Feb 28, 1982	30,000 RPM - NO LOAD - ABORTED
31	500TCP003A*BMT5	Feb 28, 1982	
32	500TCP003A*BMT1	Feb 25, 1982	
33	500TCP003C*BMT3	Feb 25, 1982	5000 RPM - NO LOAD - ABORTED
34	500TCP003*BMT4	Feb 25, 1982	5000 RPM - NO LOAD
35	500TCP003B		DAY 62

EXHIBIT 3.8.1 STATUS OF 45 mm BEARING THERMAL MODEL

	ASSIMILATION OF THERMAL PROPERTIES DATA	FINITE ELEMENT SEGMENTATION	CALCULATION OF CAPACITANCE FOR EACH NODE	CALCULATION OF CONDUCTANCE FOR EACH HEAT TRANSFER PATH	MODELING OF SIMULATED BOUNDARY CONDITIONS	CALCULATION OF HEAT GENERATION DATA	IMPLEMENTATION OF DATA INTO CARD FORMATS	RUN AND DEBUGG MODEL
ROLLING ELEMENT	✓	✓	✓	✓	✓	✓	✓	✓
CAGE	✓	✓	✓	✓	✓	✓	✓	✓
BEARING SEPARATOR	✓	✓	✓	✓	✓	✓	✓	✓
COOLANT	✓	N/A	N/A	✓	✓	N/A	✓	✓
INNER RACE	✓	✓	✓	✓	✓	✓	✓	✓
OUTER RACE	✓	✓	✓	✓	✓	✓	✓	✓
SHAFT	✓	✓	✓	✓	N/A	✓	✓	✓
IMPELLER	✓	✓	✓	✓	N/A	✓	✓	✓
HOUSING	✓	✓	✓	✓	N/A	✓	✓	✓

SRS Technologies

accomplished is shown in Exhibit 3.8.1. FORTRAN code was developed and integrated with the model to calculate approximately 100 coolant-to-metal conductors. This allows flexibility in parameterizing coolant conditions such as temperature and pressure. A temperature averaging program was also implemented to calculate the average temperature of each bearing component (inner race, rolling element, and outer race).

Estimates of heat generation for the 45 mm bearing due to ball spin, ball drag, and turbulent flow of the coolant over the inner race, outer race, separator, and cage are shown in Exhibit 3.8.2.

EXHIBIT 3.8.2. 45 MM BEARING HEAT GENERATION SUMMARY (BTU/SEC)
(12 BALL BEARINGS)

	<u>Bearing 1</u>	<u>Bearing 2</u>
Ball Spin	0.79	0.79
Ball Drag	10.08	0.38
Inner Race and Separator	0.41	0.41
Outer Race and Separator	0.16	0.16
Cage	0.15	0.15
TOTAL	<u>11.59</u>	<u>1.89</u>

A parametric analysis of the SSME 45 mm turbopump bearing was initiated during this quarter. The purpose of the analysis is to evaluate the sensitivities of coolant flow rate, inlet coolant temperature, friction factor, and axial preload. The value of each parameter to be investigated is listed in Exhibit 3.8.3. These parameter variations require 54 cases to be executed. Each case requires an iteration process between the SHABERTH model and the SINDA model to determine the bearing operating conditions for that case. Also, the effect of changing outer race tilt, outer race clearance, and heat transfer to the isolator will be studied.

EXHIBIT 3.8.3. PARAMETRIC ANALYSIS VARIATIONS

<u>PARAMETERS</u>	<u>VARIATIONS</u>
COOLANT FLOW RATE	3.6, 7.0 lbs/sec
INLET COOLANT TEMPERATURE	-240, -230, -218 (sat.) °F
FRICTION FACTOR	0.2, 0.3, 0.5
AXIAL PRELOAD	350, 480, 850 lbs

SRS Technologies

Several cases have been run during September, 1985 and the results obtained are being validated.

SRS Technologies

4.0 ANTICIPATED WORK

The parametric analysis of the operating characteristics of the LOX turbopump pump end bearing using the 45 mm bearing thermal model will continue and the present numerical instabilities will be resolved during the next reporting period. In addition, the 57 mm bearing model will be used to evaluate the effects of increased heating caused by potential cage instabilities.

The BSMT EUT data tapes will be converted into the correct format for averaging and subsequent entry into the Test Condition Data Base.

The ADORE Bearing analysis program will be used to model the dynamic characteristics of the LOX turbopump bearing.

SRS Technologies

APPENDIX A
Sample ADORE Run

```

LINNEWBIN501*ADUR2(1).TESTADORE
1 'REC 1' 1.9.50.1.0.10.5
2 'REC 2' 0.0500.0.00500.0.300.1000.DO
3 'REC 3' 1' 100M BRG 20KRPM-3.'
4 'REC 3.2' 2.1.0.18.2.0.0.3.0.0.0.0.0.0.0.0
5 'REC 3.3' 0.1.0.0.0.0.2.1.19
6 'REC 4.1' 0.100.0.1800.0.0200.0.20500. 1.00-05.5.00-05
7 'REC 4.2' 384.DO.384.DO.384.DO.384.DO.384.DO.384.DO.384.DO.384.DO
8 'REC 5A' 0.0190500.0.1400.25.DO.0.5200.0.5400
9 'REC 7.1' 0.14629200.0.13007300.0.03624100.4.735830-03.1.460500-03.0.DO
10 'REC 7.2.1' 0.13007300.0.00800.0.018120400.1.460500-03
11 'REC 7.2.2' 0.13007300.0.00800.0.018120400.1.460500-03
12 'REC 7.3' 8.63600-04.6.63600-04.0.DO.-3.00-04.0.DO
13 'REC 9.1' 4448.DO.0.DO.0.DO.0.DO.0.DO.0.DO.0.DO.0.DO.20000.DO
14 'REC 10.1' 0.00.0.02000.0.01600.1.DO
15 'REC 10.3' 1.250-07.10.DO
16 'REC 10.5.1' 0.0500.0.DO.0.DO.-0.05000.5.00-07
17 'REC 10.5.2' 0.0500. 0.DO.0.DO.-0.0500.5.00-07
18 'REC 11' 0.DO.0.DO.-9.8100

```

*YOT RUNADORE

```

AAAAAAAAA  DDDDDDDDD  000000000  RRRRRRRRR  EEEEEEEEE
AAAAAAAAA  DDDDDDDDD  00000000000  RRRRRRRRR  EEEEEEEEE
AA  AA  DD  DD  DD  DD  RR  RR  EE
AA  AA  DD  DD  DD  DD  RR  RR  EE
AA  AA  DD  DD  DD  DD  RR  RR  EE
AA  AA  DD  DD  DD  DD  RRRRRRR  EEEEEEE
AA  AA  DD  DD  DD  DD  RRRRRRR  EEEEEEE
AAAAAAAAA  DD  DD  DD  DD  RR  RR  EE
AAAAAAAAA  DD  DD  DD  DD  RR  RR  EE
AA  AA  DDDDDDDDD  00000000000  RR  RR  EEEEEEEEE
AA  AA  DDDDDDDDD  00000000000  RR  RR  EEEEEEEEE

```

-A REAL TIME SIMULATION OF ROLLING BEARING PERFORMANCE -
(VERSION ADORE-1.5)

BY
PRADEEP K. GUPTA

PROGRAM MODE = 1 SPEC CODE = 100M BRG 20KRPM-3+

BEARING TYPE = BALL

BEARING GEOMETRY

```

NO OF BALLS 18
BALL DIA (M) 1.90500-002
PITCH DIA (M) 1.40000-001
CON ANGLE (DEG) 2.50000+001

CAGE OD (M) 1.46292-001
CAGE ID (M) 1.30073-001
OUTER CLS (M) 4.73583-003
INNER CLS (M) 1.46050-003

OUTER CUR FAC 5.20000-001
INNER CUR FAC 5.40000-001
DIA PLAY (M) 2.14180-004
END PLAY (M) 9.66105-004

CAGE WIDTH (M) 3.62410-002
POC DIA CL (M) 8.63600-004
GUIDE LAND TYPE 2 2

OUTER FIT (M) 1.00000-005
INNER FIT (M) 5.00000-005

LAND DIA (M) 1.30073-001
LAND CLS (M) 1.46050-003
LAND POS (M) 1.81204-002

SHAFT OD (M) 1.00000-001
SHAFT ID (M) 2.00000-002
BEARING OD (M) 1.80000-001
HOUSING OD (M) 2.05000-001

LAND WIDTH (M) 8.00000-003
LAND POS (M) 1.81204-002

```

MATERIAL PROPERTIES

	DENSITY (KGM/M**3)	ELASTIC MODULUS (PA)	POISSON-S RATIO	COEFF OF THER EXP (1/K)	HARDNESS (PA)	WEAR COEFFICIENT
SHAFT	7.75037+003	1.99948+011	2.50000-001	1.17000-005		
HOUSING	7.75037+003	1.99948+011	2.50000-001	1.17000-005		
ROLL ELE	7.75037+003	1.99948+011	2.50000-001	1.17000-005	7.84532+009	5.00000-006
RACE	7.75037+003	1.99948+011	2.50000-001	1.17000-005	7.84532+009	5.00000-006
CAGE	7.75037+003	1.99948+011	2.50000-001	1.80000-005	7.84532+008	5.00000-004

INERTIAL PARAMETERS

	MASS (KGM)	MOMENT OF INERTIA (KGM*M*2)		MASS TO GEO CENTER (M)			
		X-COMP	Y-COMP	Z-COMP	X-COMP	Y-COMP	Z-COMP
RE	2.80547-002	1.01811-006	1.01811-006	1.01811-006	.00000	.00000	.00000
CAGE	6.36472-001	3.04873-003	1.59403-003	1.59403-003	.00000	.00000	.00000

LUBRICATION PARAMETERS

CRITICAL FILM AT ZERO SLIP (M)	TRAC COEFF	MAXIMUM TRAC COEFF	TRAC COEFF AT INF SLIP	SLIP AT MAX TRACTION (M/S)	COEFFICIENT A (S/M)	COEFFICIENT B (S/M)	COEFFICIENT C (S/M)	COEFFICIENT D
RE/RACE	1.25000-007	.00000	2.00000-002	1.60000-002	1.00000+000	.00000	.00000	-5.00000-002
RE/CAGE	5.00000-007				5.00000-002	.00000	.00000	-5.00000-002
CAGE/RACE	5.00000-007				5.00000-002	.00000	.00000	

LUBRICANT CODE..... 3 MIL-L-7808

FILM THICKNESS CODE... 2

REF TEMP (K)	EFF DENSITY (KGM/M*3)	VISCOCITY (PA*S)	PR-VIS COEFFICIENT (1/PA)	TEMP-VIS COEFF TYPE 1 (1/K)	TEMP-VIS TYPE 2 (K)	THERMAL CONDUCTIVITY (N/S/K)	STARVATION PARAMETER	REF ROLLING VELOCITY (M/S)
LUB FILM	3.84000+002	2.40129-003	7.13543-009	2.29719+003	2.29719+003	9.65790-002	1.00000+001	2.54000+001
TRACTION	3.84000+002	1.03289-002	5.22140-009	4.69196-002	4.69196-002			

INITIAL OPERATING CONDITIONS

```

APPL AXIAL LOAD      (N)  4.44800+003
APPL RADIAL DISP     (M)  .00000
SHAFT TEMP           (K)  3.84000+002
HOUSING TEMP         (K)  3.84000+002
ROLL ELE TEMP        (K)  3.84000+002
ROOM TEMP            (K)  3.84000+002

CAGE POS...AXIAL     (M)  .00000
...RADIAL            (M) -3.00000-004
...ANGULAR (RAD)     .00000
  
```

SCALE FACTORS AND OUTPUT CONTROLS

```

.....SCALE FACTORS.....
LENGTH      (M)  9.52500-003
LOAD        (N)  4.44800+003
TIME        (S)  2.45106-004
  
```

```

          OUTER RACE  INNER RACE
ANGULAR VELOCITY (RPM)  2.00000+004
TEMPERATURE      (K)   3.84000+002
MISALIGNMENT-Y   (RAD)  .00000
MISALIGNMENT-Z   (RAD)  .00000
TRANSLATIONAL CONSTRAINTS  1  1  1  1  1
ROTATIONAL CONSTRAINTS    1  1  1  1  1

GRAVITY VECTOR (M/S**2)  .00000
CAGE TEMPERATURE (K)    3.84000+002
  
```

```

.....STEP SIZE INFO.....
MINIMUM      5.00000-003
MAXIMUM      3.00000-001
INITIAL      5.00000-002
ERROR LIMIT  1.00000-006
  
```

```

          NO OF STEPS
          DATA CONTROL  9  50
          AUTO PLOTS    1  19
                      0  0
          INT METHOD     5  0
          TRACTION INT  0  0
  
```

OUTPUT FROM USER ACCESSIBLE ROUTINES ---

STEP NO	TAU	TIME (S)	OUTER RACE ROT (DEG)	INNER RACE ROT (DEG)
0	.000	.000	.000	.000

100M BRG 20KRPM-3*

1. ROLLING ELEMENT PARAMETERS

RE NO	ORBITAL POSITION (DEG)	CONTACT ANGLE (DEG)	CONTACT LOAD (N)	CONTACT STRESS (PA)	MAJOR HALF WIDTH (M)	MINOR HALF WIDTH (M)
1	0.000	2.571+001	2.279+003	1.538+009	1.130-003	3.065-004
10	1.800+002	2.571+001	2.279+003	1.538+009	1.130-003	3.065-004

RE NO	ORBITAL VELOCITY (RPM)	ANGULAR VELOCITY (RPM)	RE ANG POSITION (DEG)	SPIN/ROLL (DEG)	CONTACT LOSS (N*M/S)	TIME AVE WEAR RATE (M*3/S)
1	9.017+003	7.555+004	-5.484+000	1.800+002	2.312+000	9.943-013
10	9.017+003	7.555+004	-5.484+000	1.800+002	2.312+000	9.943-013

RE NO	SLIP VELOCITY (M/S)	TRAC COEFF	ISO LUB FILM (M)	THERMAL RED FAC (N)	DRAG (N*M)	NET LOSS (N*M/S)
1	-2.311-001	-6.741-017	-5.061-003	4.137-007	6.238-001	6.465-001
10	-2.311-001	-6.741-017	-5.061-003	4.137-007	6.238-001	6.465-001

STEP NO 0
 TAU .000
 TIME (S) .000
 OUTER RACE ROT (DEG) .000
 INNER RACE ROT (DEG) .000
 100M BRG 20KRPM-3*

2. RACE AND CAGE PARAMETERS

RE												
NO		GEO INT		RACE/CAGE		INTERACTION		CONTACT		TIME AVE		
		(M)		FORCE (N)		ANGLE (DEG)		LOSS (N*M/S)		WEAR RATE (M**3/S)		
1	4.318-004		.000		.000		.000		.000		.000	
2	3.292-004		.000		.000		.000		.000		.000	
3	2.390-004		.000		.000		.000		.000		.000	
4	1.720-004		.000		.000		.000		.000		.000	
5	1.364-004		.000		.000		.000		.000		.000	
6	1.364-004		.000		.000		.000		.000		.000	
7	1.720-004		.000		.000		.000		.000		.000	
8	2.390-004		.000		.000		.000		.000		.000	
9	3.292-004		.000		.000		.000		.000		.000	
10	4.318-004		.000		.000		.000		.000		.000	
11	3.292-004		.000		1.800+002		.000		.000		.000	
12	2.390-004		.000		1.800+002		.000		.000		.000	
13	1.720-004		.000		1.800+002		.000		.000		.000	
14	1.364-004		.000		1.800+002		.000		.000		.000	
15	1.364-004		.000		1.800+002		.000		.000		.000	
16	1.720-004		.000		1.800+002		.000		.000		.000	
17	2.390-004		.000		1.800+002		.000		.000		.000	
18	3.292-004		.000		1.800+002		.000		.000		.000	

LAND		RACE/CAGE		FORCES		RACE/CAGE		EFFECTIVE		CONTACT		TIME AVE	
NO		(N)		(DEG)		(DEG)		(M)		(N*M/S)		(M**3/S)	
		NORMAL		TRACTION		CON ANGLE		SLIP VEL (M/S)		DIA PLAY (M)		WEAR RATE (M**3/S)	
1	.000		.000		.000		.000		3.935-004		1.387-003		.000
2	.000		.000		.000		.000		3.935-004		1.387-003		.000

MASS CENTER POSITION													
AXIAL (M)		RADIAL (M)		ORBITAL (DEG)		VELOCITY (RPM)		AMPLITUDE (RPM)		ANGULAR VELOCITY		ANG POSITION	
										PHI (DEG)		THETA (DEG)	
CAGE	-1.181-004	3.000-004	1.800+002	9.017+003	9.017+003	.000	.000	.000	.000	.000	.000	3.552+007	.000
ORACE	.000	.000	.000	.000	.000	.000	.000	.000	.000	.000	.000	-6.400+006	8.594-012
IRACE	-1.064-004	.000	.000	.000	2.000+004	.000	.000	.000	.000	.000	.000	1.183+008	9.303-012

STEP NO	TAU	TIME (S)	OUTER RACE ROT (DEG)	INNER RACE ROT (DEG)	100M BRG 20KRPM-3*
0	.000	.000	.000	.000	

3. APPLIED PARAMETERS

APPLIED FORCES		APPLIED MOMENTS		BASIC FATIGUE LIFE		
(N)	COMP-X	(N)	COMP-Z	(N*M)	COMP-Z	(HOURS)
CAGE	.000	-6.244+000	.000	.000	.000	4.100+002
ORACE	4.448+003	1.669-013	-3.858-013	-1.112+000	-2.756-015	1.125-004
IRACE	-4.448+003	-1.760-014	8.198-014	-9.794-002	2.738-015	5.000-006
						4.883-007
						5.944+001
						.000

4. TIME STEP SUMMARY

STEP NO	TIME (S)	OUTER RACE ROTATION (DEG)	INNER RACE ROTATION (DEG)	TIME AVERAGE PARAMETERS			
				FATIGUE LIFE (HOURS)	POWER RE ORBITAL LOSS (N*M/S)	CAGE OMEGA RATIO	WHIRL CAGE WEAR RATE (M**3/S)
0	.000	.000	.000	4.100+002	5.944+001	4.509-001	4.509-001
							.000

STEP NO	TAU	TIME (S)	OUTER RACE ROT (DEG)	INNER RACE ROT (DEG)	100M BRG 20KRPM-3*
10	1.435+000	3.516-004	.000	4.220+001	=====
---	=====	=====	=====	=====	=====

1. ROLLING ELEMENT PARAMETERS

RE NO	ORBITAL POSITION (DEG)	CONTACT ANGLE (DEG)	CONTACT LOAD (N)	CONTACT STRESS (PA)	MAJOR HALF WIDTH (M)	MINOR HALF WIDTH (M)
1	1.903+001	6.225+000	2.279+003	1.538+009	2.309-003	1.130-003
10	1.990+002	6.225+000	2.279+003	1.538+009	2.309-003	1.130-003

1	OUTER RACE	INNER RACE	OUTER RACE	INNER RACE	OUTER RACE	INNER RACE
1	1.903+001	6.225+000	2.279+003	1.538+009	2.309-003	1.130-003
10	1.990+002	6.225+000	2.279+003	1.538+009	2.309-003	1.130-003

RE NO	ORBITAL VELOCITY (RPM)	AMPLITUDE (RPM)	ANGULAR VELOCITY (DEG)	THETA (DEG)	PHI (DEG)	RE ANG POSITION (DEG)	SPIN/ROLL (N*M/S)	CONTACT LOSS (M*3/S)	WEAR RATE (M*3/S)
1	9.018+003	7.554+004	-5.423+000	5.222+000	1.628+002	4.958+003	3.867-001	4.181+001	7.180+000
10	9.018+003	7.554+004	-5.423+000	5.222+000	1.628+002	4.958+003	3.867-001	4.181+001	7.180+000

1	OUTER RACE	INNER RACE	OUTER RACE	INNER RACE	OUTER RACE	INNER RACE
1	9.018+003	7.554+004	-5.423+000	5.222+000	1.628+002	4.958+003
10	9.018+003	7.554+004	-5.423+000	5.222+000	1.628+002	4.958+003

RE NO	SLIP VELOCITY (M/S)	TRAC COEFF	ISO LUB FILM (M)	THERMAL RED FAC	DRAG (N)	CHUR MOM (N*M)	NET LOSS (N*M/S)
1	-1.845-001	-1.431-001	-1.961-003	-8.577-004	4.453-007	6.225-001	6.450-001
10	-1.855-001	-1.442-001	-1.972-003	-8.640-004	4.453-007	6.225-001	6.450-001

STEP NO	TAU	TIME (S)	OUTER RACE ROT (DEG)	INNER RACE ROT (DEG)
10	1.435+000	3.516-004	.000	4.220+001

100M BRG 20KRPM-3*

2. RACE AND CAGE PARAMETERS

RE NO	GE0 INT (M)	RE/CAGE CONTACT FORCE (N)	CONTACT ANGLE (DEG)	CONTACT LOSS (N*M/S)	TIME AVE WEAR RATE (M**3/S)
1	4.293-004	.000	.000	.000	.000
2	3.214-004	.000	.000	.000	.000
3	2.270-004	.000	.000	.000	.000
4	1.574-004	.000	.000	.000	.000
5	1.211-004	.000	.000	.000	.000
6	1.224-004	.000	.000	.000	.000
7	1.612-004	.000	.000	.000	.000
8	2.327-004	.000	.000	.000	.000
9	3.284-004	.000	.000	.000	.000
10	4.268-004	.000	.000	.000	.000
11	3.189-004	.000	.000	.000	.000
12	2.245-004	.000	.000	.000	.000
13	1.549-004	.000	.000	.000	.000
14	1.186-004	.000	.000	.000	.000
15	1.199-004	.000	.000	.000	.000
16	1.587-004	.000	.000	.000	.000
17	2.303-004	.000	.000	.000	.000
18	3.260-004	.000	.000	.000	.000

LAND NO	NORMAL (N)	RACE/CAGE TRACTION (N)	FORCES (DEG)	CON ANGLE (DEG)	ATT ANGLE (DEG)	RACE/CAGE GEO INT (M)	RACE/CAGE SLIP VEL (M/S)	EFFECTIVE DIA PLAY (M)	CONTACT LOSS (N*M/S)	TIME AVE WEAR RATE (M**3/S)
1	.000	.000	1.902+001	.000	.000	3.768-004	.000	1.387-003	.000	.000
2	.000	.000	1.902+001	.000	.000	3.768-004	.000	1.387-003	.000	.000

CAGE ORACE IRACE	AXIAL (M)	CENTER RADIAL (M)	POSITION ORBITAL (DEG)	VELOCITY (RPM)	ORBITAL VELOCITY (RPM)	AMPLITUDE (RPM)	ANGULAR VELOCITY THETA (DEG)	PHI (DEG)	ANG POSITION THETA (DEG)	PHI (DEG)	HOOP STRESS (PA)	TIME AVE WEAR RATE (M**3/S)
-1.181-004	3.167-004	1.983+002	8.076+003	9.017+003	.000	.000	.000	.000	.000	.000	3.552+007	.000
.000	.000	.000	.000	.000	.000	.000	.000	.000	.000	.000	-6.400+006	2.913-011
-1.064-004	.000	.000	.000	2.000+004	.000	.000	.000	.000	.000	.000	1.183+008	1.216-011

STEP NO	TAU	TIME (S)	OUTER RACE ROT (DEG)	INNER RACE ROT (DEG)	100M BRG 20KRPM-3*
10	1.435+000	3.516-004	.000	4.220+001	

3. APPLIED PARAMETERS

APPLIED FORCES		APPLIED MOMENTS		BASIC FATIGUE LIFE	
(N)	(N)	(N)	(N)	(HOURS)	(M)
COMP-X	COMP-Y	COMP-X	COMP-Y	INTERNAL CLEARANCE	3.730+002
COMP-Z	COMP-Z	COMP-X	COMP-Y	OUTER RACE FIT	1.125-004
		COMP-Z	COMP-Z	INNER RACE FIT	5.000-006
					4.883-007
				TOTAL POWER LOSS	8.819+002
				CHURNING LOSS FRACTION	.000

4. TIME STEP SUMMARY

STEP NO	TIME (S)	OUTER RACE ROT (DEG)	INNER RACE ROT (DEG)	FATIGUE LIFE (HOURS)	TIME AVERAGE PARAMETERS			
					POWER RE ORBITAL CAGE LOSS (N*M/S)	OMEGA CAGE WHIRL RATIO	WEAR RATE (M**3/S)	CAGE
10	3.516-004	.000	4.220+001	3.737+002	4.044+002	4.509-001	4.344-001	.000

EXECUTION COMPLETED
EXIT FROM -ADORE- DUE TO MAXIMUM STEP COUNT

STATISTICS OF THIS RUN

MINIMUM STEP SIZE	= 5.00000-002
MAXIMUM STEP SIZE	= 1.56758-001
LAST STEP SIZE	= 1.56758-001
MAX AVE TRUNCATION	= 3.17891-007
TOTAL DERIVATIVE CALLS	= 81

*BRKPT PRINT\$

UNSMSC HCC

NAME- LINNEW

DIST. CODE-BIN501

RUN ID- SPECTR

JOB NO- 6EH553450050

SEQ NO- SPECTT

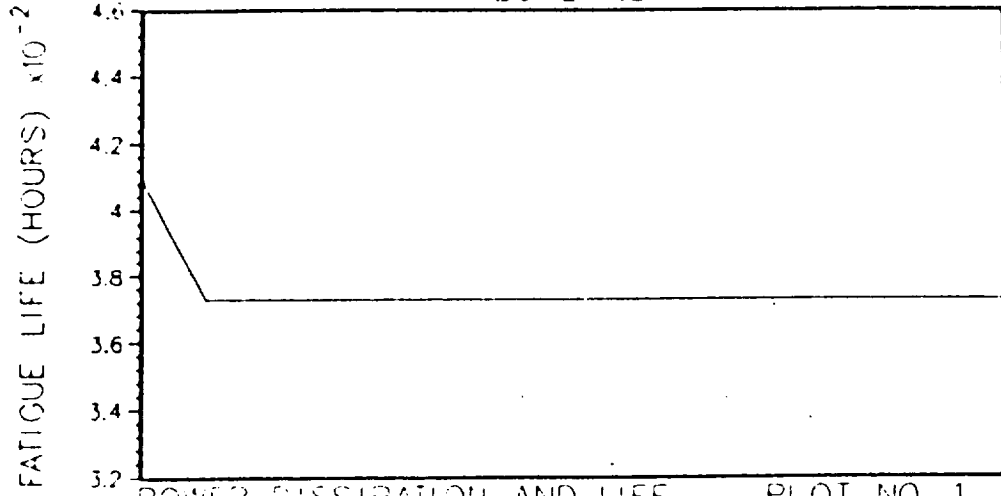
DATE- 081285

TIME- 161135

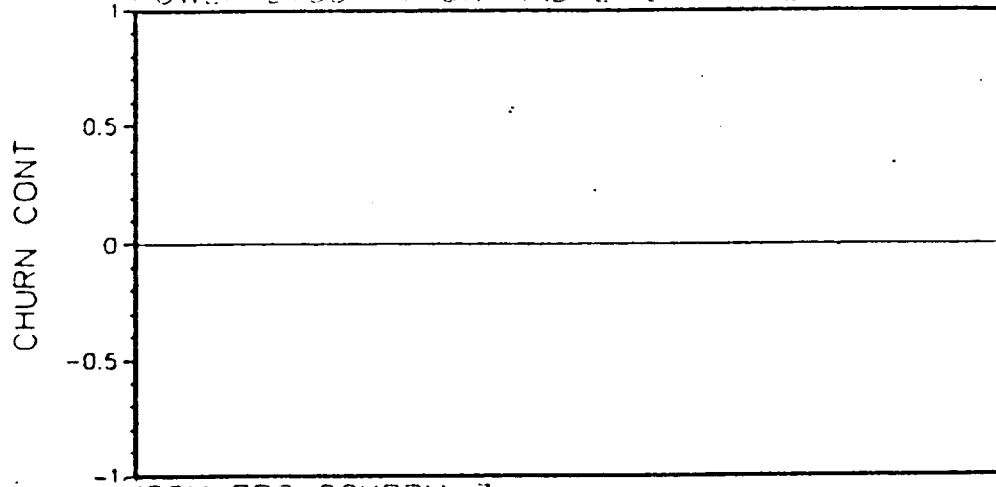
OF POOR QUALITY

ADVANCED DYNAMICS OF ROLLING ELEMENTS

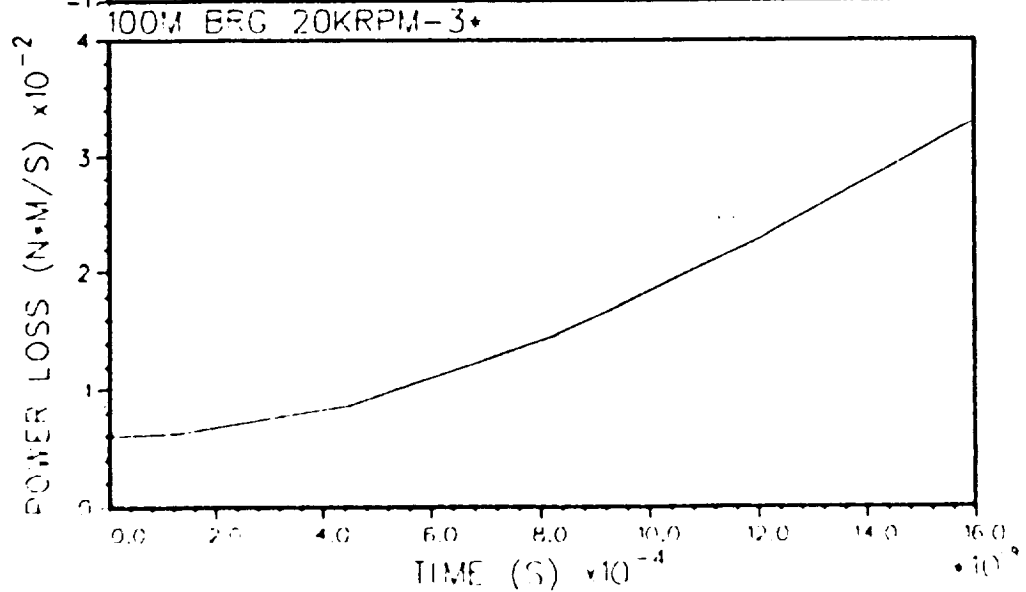
ADORE-1.5



M= 3.74+000
S= 5.75+000



M= .00
S= .00

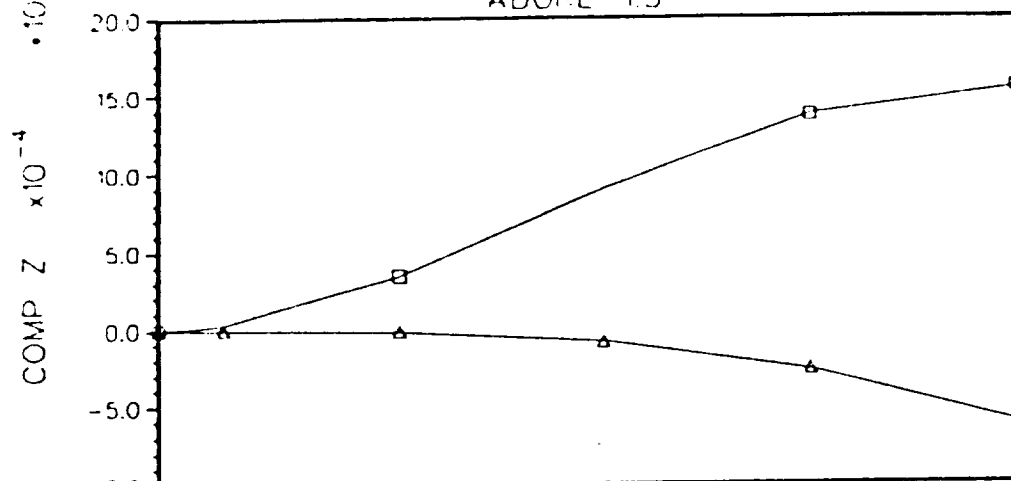


M= 1.60+000
S= 8.22+000

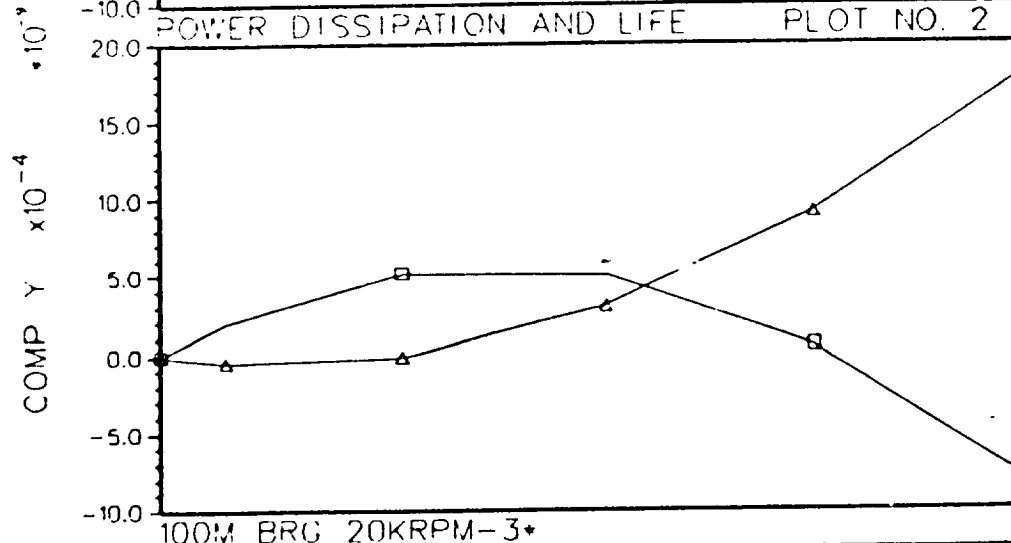
ADVANCED DYNAMICS OF ROLLING ELEMENTS

ADOPE-1.5

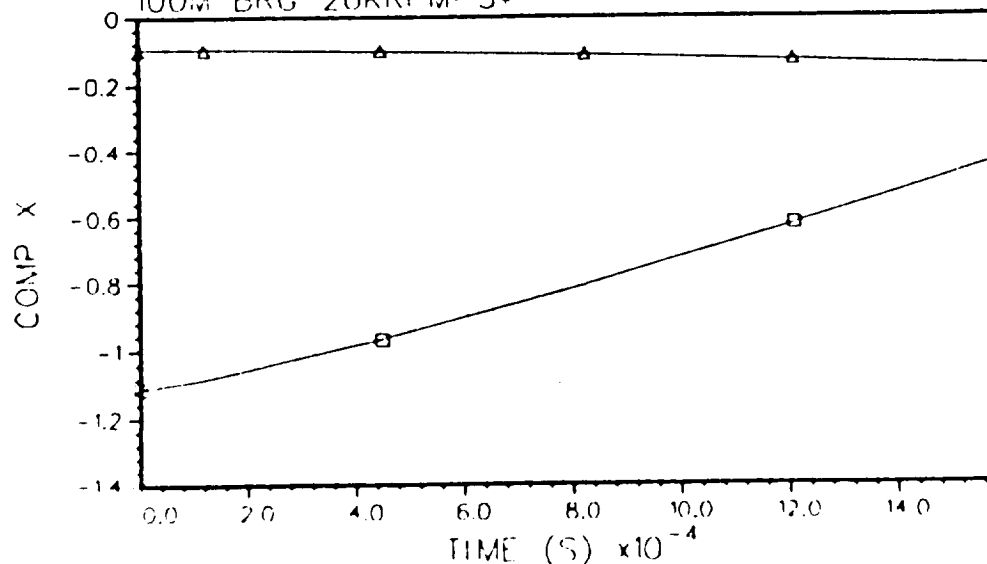
.....APPLIED MOMENT ON THE RACES (N•M)

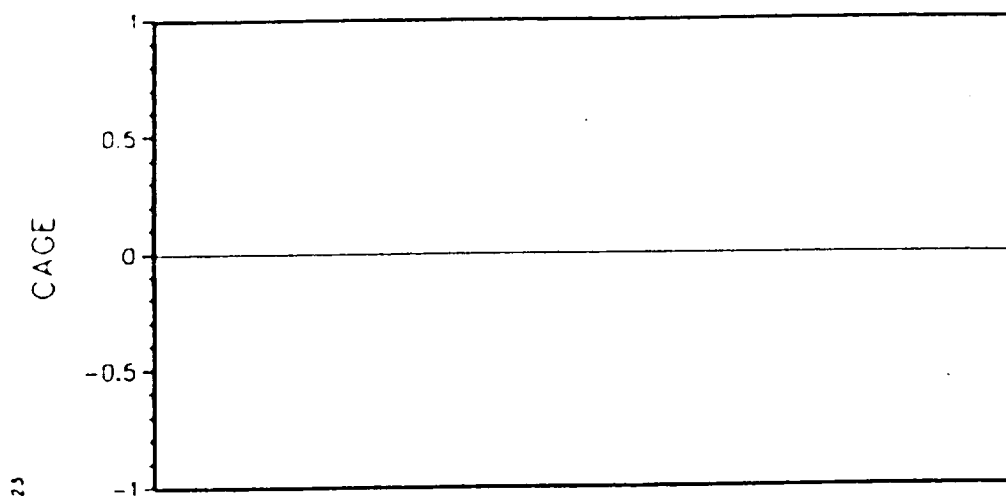


POWER DISSIPATION AND LIFE PLOT NO. 2

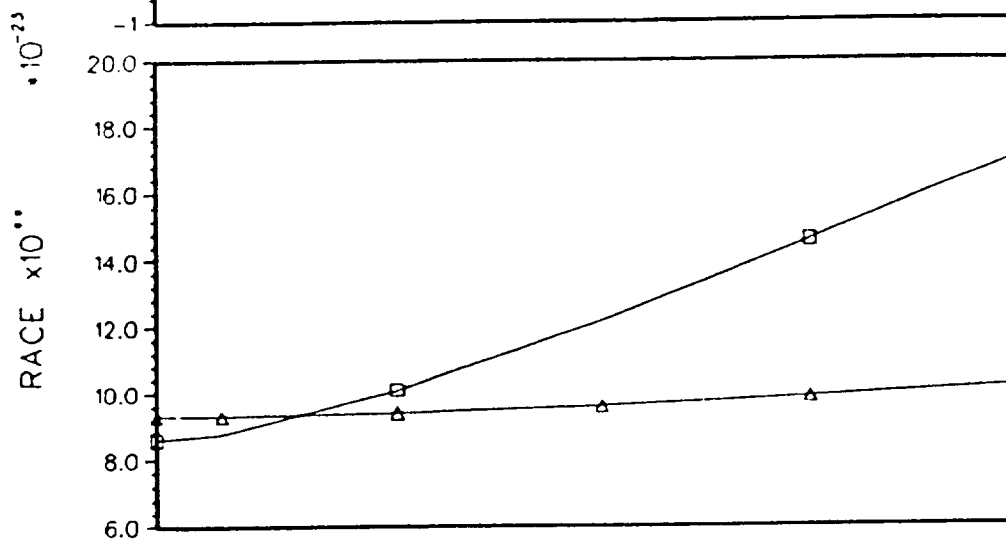


100M BRG 20KRPM-3*





M= .00
S= .00



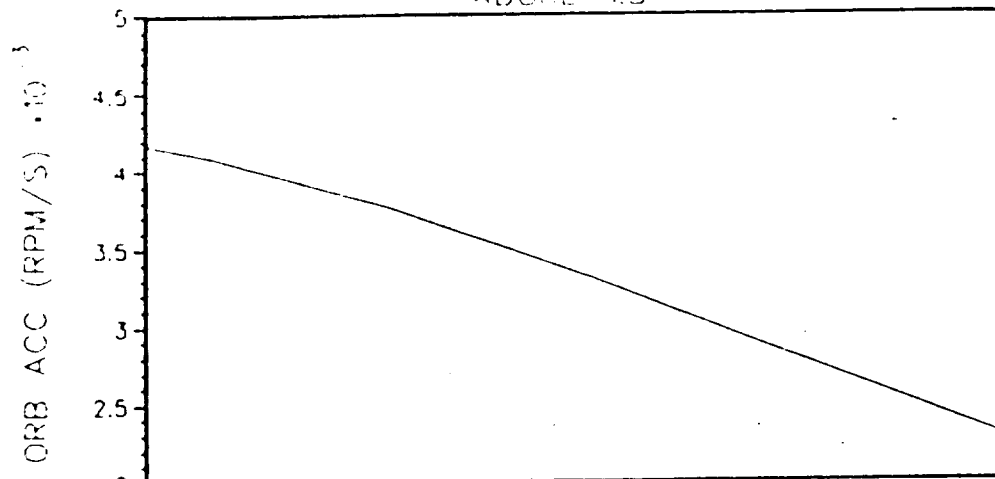
LEGEND

□ = OUTER RACE
M= 1.23-011
S= .00

△ = INNER RACE
M= 9.64-012
S= .00

ADVANCED DYNAMICS OF ROLLING ELEMENTS

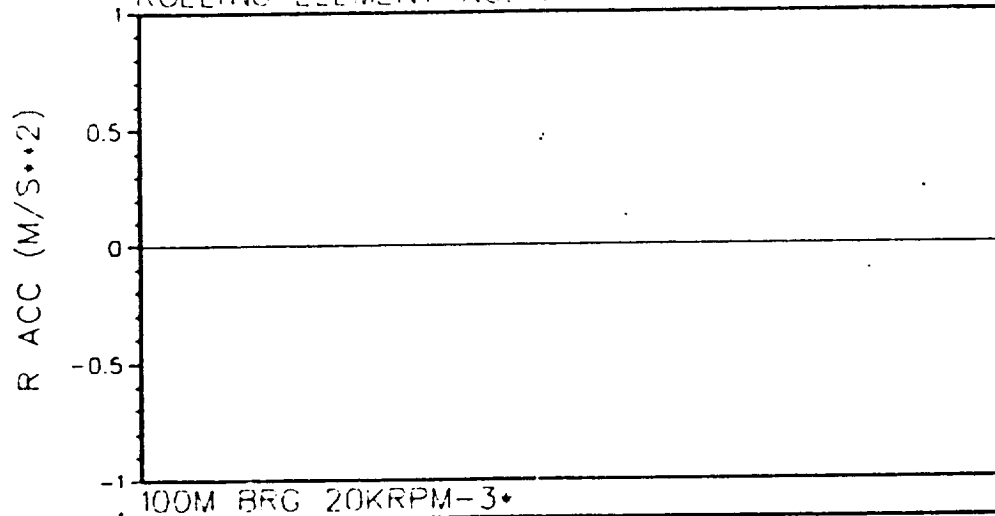
ADORE-1.5



ROLLING ELEMENT NO. 1

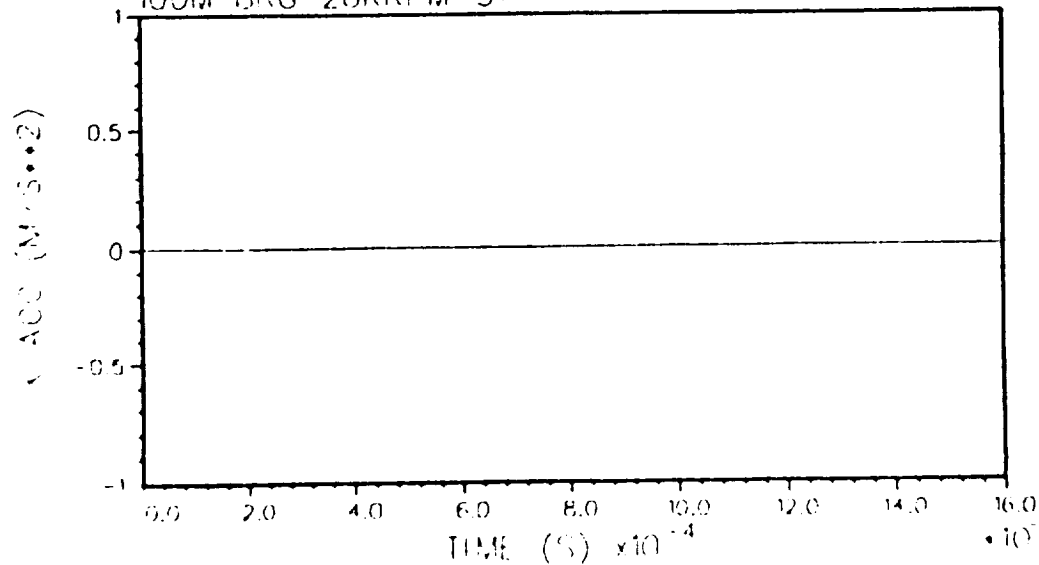
PLOT NO. 1

M= 3.31+003
S= 5.61+002



100M BRG 20KRPM-3*

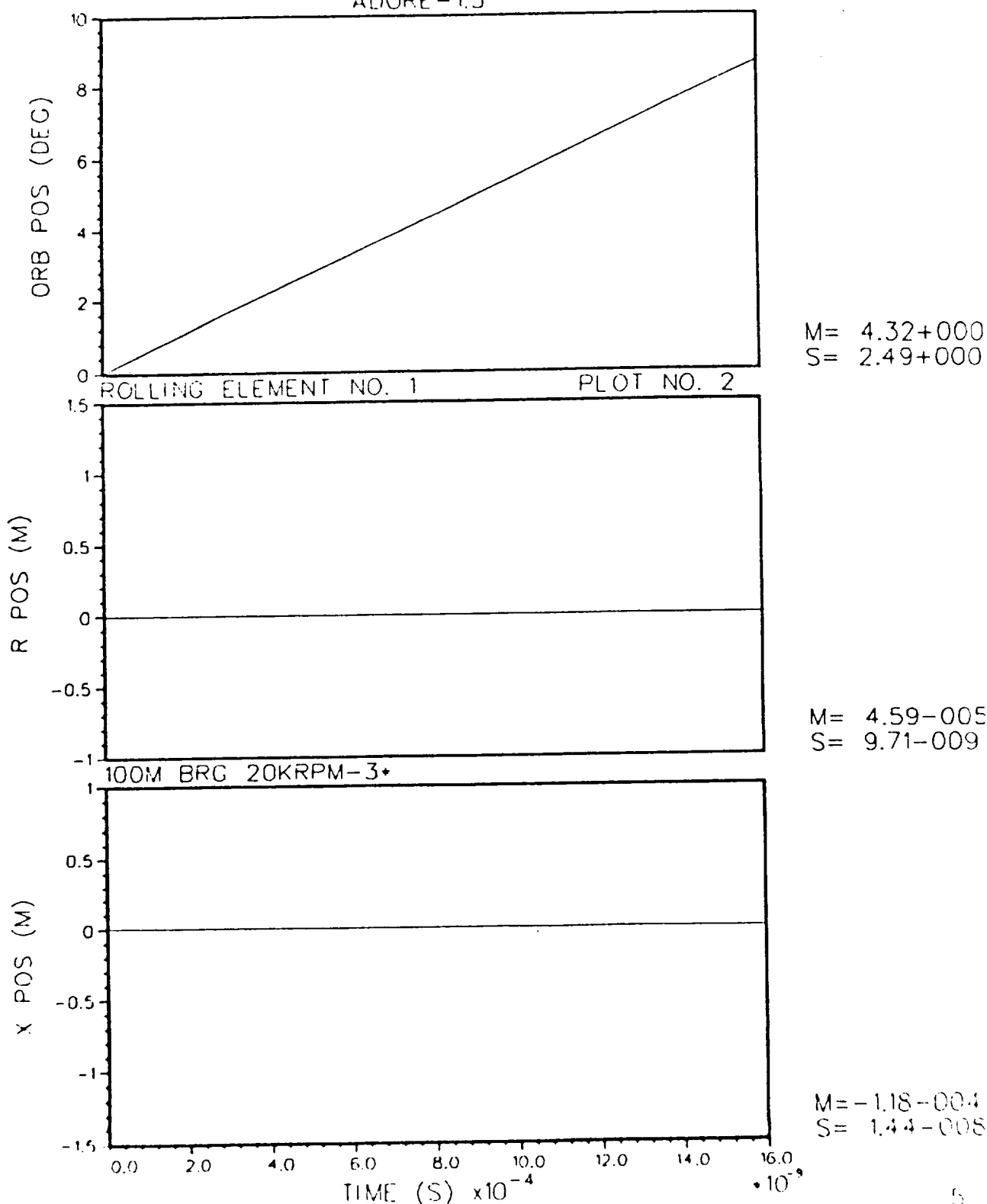
M= .00
S= .00



M= .00
S= .00

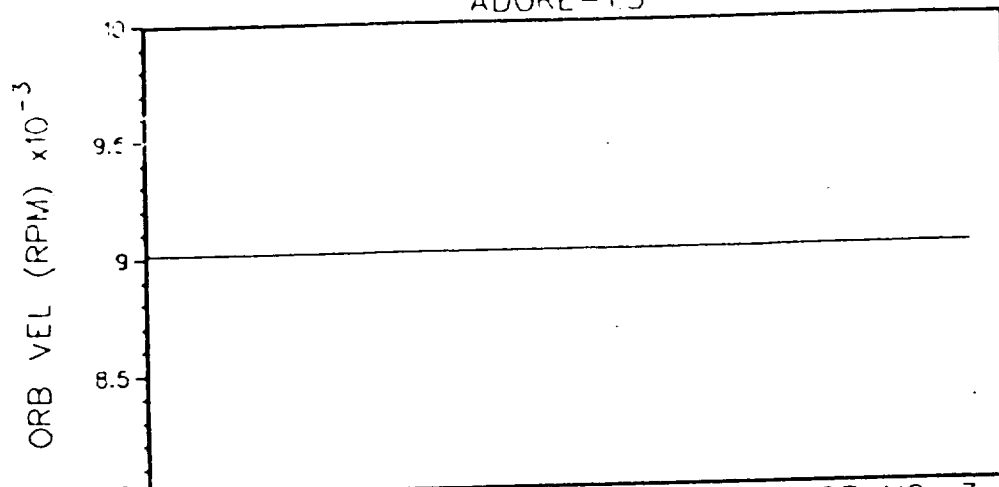
ADVANCED DYNAMICS OF ROLLING ELEMENTS

ADORE-1.5

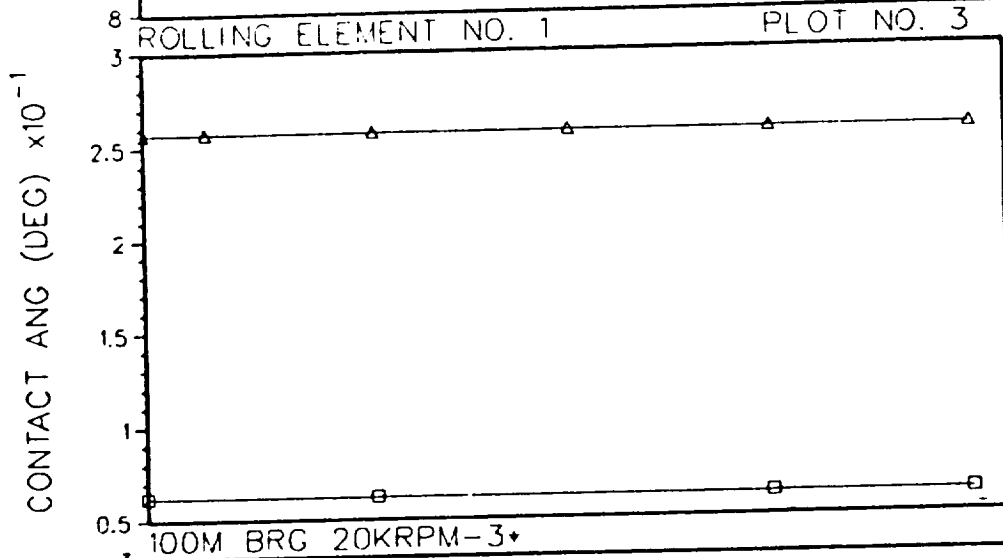


ADVANCED DYNAMICS OF ROLLING ELEMENTS

ADORE-15



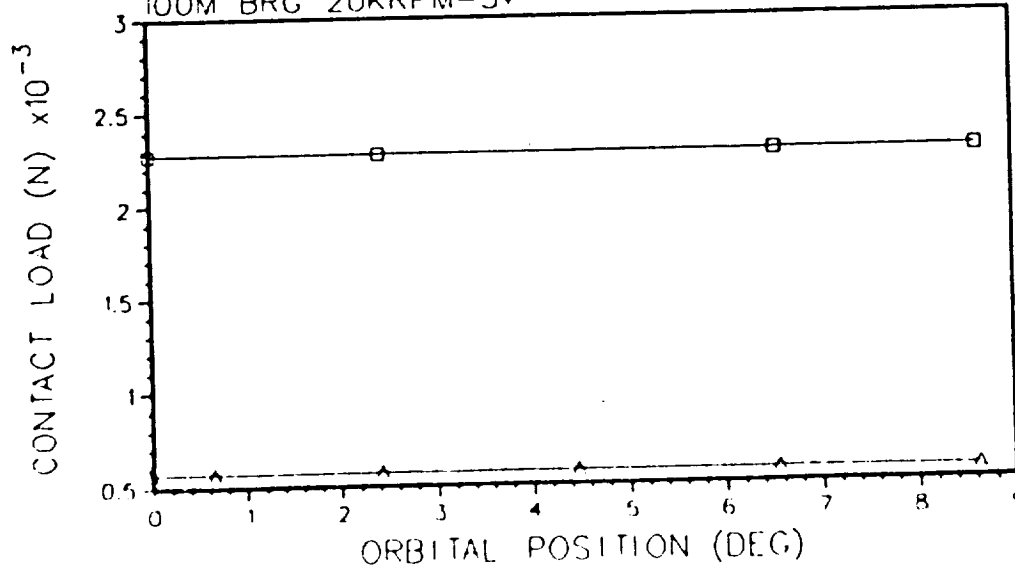
M= 9.02+003
S= 1.10+000



LEGEND

□ = OUTER RACE
M= 6.23+000
S= 1.32-003

△ = INNER RACE
M= 2.57+001
S= 3.14-003



LEGEND

□ = OUTER RACE
M= 2.28+003
S= 2.78-001

△ = INNER RACE
M= 5.70+002
S= 1.70-001

DISTRIBUTION: George C. Marshall Space Flight Center

Mr. Fred J. Dolan, EH14 (6 Copies + Repro)

Mr. Schwinghamer, EH01

Mr. Riggs, EP23

Mr. McCarty, EP21

Mr. Geotz, EE51

Mr. Lombardo, SA53

Mr. G. Smith, SA51

Mr. Lovingood, SA51

AT01

AS24D (3 Copies)

EH11

AP29-F

EM13B-21

BF30

CC01/Wofford

NASA Lewis Research Center

Mr. Huberty W. Scibbe, Mail Stop 23-2

Mr. R. W. Parker, Mail Stop 23-2

Mr. Ned P. Hannum, Mail Stop 501-6

NASA Headquarters

Mr. F. W. Stephenson, Code RST-5/E

Mr. M. Greenfield, Code RTM-6

NASA Scientific and Technical Information Center

ATTN: Accessioning Department (1 Copy + Repro)

DCASMA